EFFECTS OF AMERICAN COLONIAL SETTLEMENT AND DEFORESTATION ON LACUSTRINE REDOX CONDITIONS: LONGTERM INSIGHTS FROM MARTIN LAKE, INDIANA

Alyssa Nicole Henke

Submitted to the faculty of the University Graduate School
in partial fulfillment of the requirements
for the degree
Master of Science
in the Department of Earth Sciences,
Indiana University

November 2020

Accepted by the Graduate Faculty of Indiana University, in partial fulfillment of the requirements for the degree of Master of Science.

Master's Thesis Committee

_____

William Gilhooly, III, PhD, Chair

_____

Broxton Bird, PhD

_____

Gregory Druschel, PhD

DEDICATION

For Grant, whose support throughout this degree was irreplaceable.

ACKNOWLEDGEMENT

I would like to acknowledge Dr. William Gilhooly, III for his dedication and commitment to higher education. Without his unwavering confidence and patience in me and this project this research could have never been completed. He saw potential and elevated me academically and professionally to a spot I never thought I would be and for that I am truly grateful. I would also like to thank my other committee members Dr. Greg Druschel and Dr. Broxton Bird, whose expertise, mentorship, and review throughout was fundamental to my success. In addition, I thank Derick Gibson, who without his help in collecting samples this project could have never came to fruition. Additional data for this project was obtained thanks to Dr. Jeremy Owens. My parents deserve all the thanks in the world for raising me with a love of knowledge and providing me with an amazing life and the luxury to pursue a higher education.

Alyssa Nicole Henke

EFFECTS OF AMERICAN COLONIAL SETTLEMENT AND DEFORESTATION ON LACUSTRINE REDOX CONDITIONS: LONGTERM INSIGHTS FROM MARTIN LAKE, INDIANA

Colonial settlement of Indiana changed the environment in significant ways; the aim of this study is to quantify the impacts of settlement through the use of geochemical proxies including: % lithics; the carbon ($\delta^{13}C$), nitrogen ($\delta^{15}N$), and sulfur ($\delta^{34}S$) isotope composition of organic matter; the elemental composition of carbon (TOC) and nitrogen (N_{tot}) in organic matter and their ratio (C/N); the $\delta^{34}S$ of mineral sulfides (pyrite and acid volatile sulfides); and iron redox proxies. Lakes are a great recorder of aquatic-terrestrial linkages on both local and global scales. Martin lake's watershed, in northeastern Indiana, was settled in 1840 by Euro-Americans, and since then clear shifts in lake chemistry are recorded in its sediments.

A core spanning roughly the last 300 years taken from Martin Lake is the basis of this study. The impacts of settlement can be seen through the lenses of all the proxies that were used in this study. **1**) Post-settlement deforestation increased erosion in Martin Lake's watershed, increasing sedimentation rates and % lithics. **2**) $\delta^{13}C$ of organic matter reveals a pattern of deforestation and partial regrowth and agricultural use of land. **3**) A pronounced increase in $\delta^{15}N$ timed with the change in population at the time of settlement is consistent with the increased input of human or animal waste into Martin Lake. **4**) TOC and C/N show an overall increase in the amount of organic matter within the lake caused by deforestation, and that the increased nutrient supply may have stimulated more in-lake productivity. **5**) $\delta^{34}S$ of mineral sulfides show that deforestation lead to an increase in the available sulfate pool of Martin Lake, which in combination with **6**) an increase in Fe_{HR} created redox conditions in which pyrite formation was more favorable. These factors culminated in a transition in Martin Lake chemistry and redox cycling within the sediments.

William Gilhooly, III, PhD, Chair

TABLE OF CONTENTS

LIST OF TABLES

LIST OF FIGURES

CHAPTER 1

1.1 Native Americans and Pre-Indiana: The Settlement of Indiana

The landscape that is now Indiana has been habited by humans since the end of the Wisconsin glacial maximum (12,000-10,000 Before Common Era; BCE) (Cochran, 2004). Paleoindians of this time period are characterized as small family bands that migrated over territory as vast as 5150 km^2 (Wobst, 1976) in search of large game animals (Cochran, 2004). Upon the retreat of the glaciers, Indiana's landscape changed, and new cultures emerged, termed the Archaic cultures (8000-1000 BCE), which began adapting to the warming climate (Cochran, 2004). The Woodland cultures emerged in 1000 BCE with a large cultural shift with the development of pottery and the beginning of horticulture. These peoples continued to practice hunting and gathering for subsistence, but the beginning of the cultivation of native and exotic plants can be seen. The cultivation of corn was introduced to the Midwest near the end of this period (approximately 900 Common Era; CE) although this practice was heavily centralized in the river valley areas (Cochran, 2004). Large urban centers were developed in the region between 1000-1200 CE, as Native Americans of the region adopted an intensive maize agriculture system that was able to support such population growth (Bird et al., 2017). The climatic conditions in Indiana during the beginning of the Mississippian period (1200- 1540 CE) changed from a post-glacial warm and wet climate to a much drier climate. The ensuing drier conditions in 1250-1350 CE, coincided with socio-political instability and increased warfare as the maize agriculture they relied upon began to collapse due to water scarcity (Bird et al., 2017). By 1350-1450 CE, particularly severe warm season droughts caused the final breakdown of the civilization and the relocation of its remaining people to more southern locations (Bird et al., 2017), which approximately coincides with the beginning of the Late Mississippian period (Cochran, 2004).

Although various Native American groups have occupied Indiana for thousands of years, at the point of Euro-American contact (in the late 1700's), Indiana was relatively vacant of native people compared to previous periods (Cochran, 2004). The period of time in which colonial settlers interacted with the Native Americans, in what is

present day Indiana, was limited before the Revolutionary War when some Native Americans settled near French trading posts along the Wabash River (Sieber and Munson, 1992). After the Revolutionary War ended, The Land Act of 1800 encouraged colonist to settle in the area in far greater numbers. The first land office was opened at Vincennes in 1807 (Carman, 2013). Although Indiana was made an official territory of the United States in 1800, Native Americans controlled two-thirds of the land at that time. This stood until the Battle of Tippecanoe in 1811 when the Shawnee Tribe was defeated, which lead to a weakened dominance for other Native American tribes who eventually surrendered their land through treaties and were forced to migrate further west (Jenkins, 2013). In 1816 Indiana officially gained statehood, and colonial population growth increased even faster than before (Sieber and Munson, 1992). LaGrange County, where Martin Lake is located, was officially settled in 1832 by New Englanders and, by 1840, the population had grown to over 3,600 (Cox, 1873).

1.2 Disturbance of the Natural Landscape

Pre-Columbian population density of Native Americans is largely unknown at a finer scale for most geographic regions; however, the Native American population of the continental United States as of the 1800s is estimated at 600,000, and decreased substantially over the decades (Thornton, 2000). Pre-Columbian Native Americans were skilled with tools and used them to better shape their environment to suit their needs. They cleared forest for agricultural use through the processes of burning and tree deadening (a process in which the outer bark is completely removed in a strip around the tree). Although this damage was likely localized and limited in time, over centuries it probably created a landscape of varied stand ages and forest types as areas were cleared, cultivated, and abandoned (Jenkin, 2004). Late Mississippian cultures forgoed large permanent population centers and stayed mobile. Although they did not have dense populations, they likely affected local resources through the collection of firewood and fruits/nuts (Jenkins, 2004).

Colonial settlers adopted the clear-cut methods of the Native Americans such that 41 years after the official settlement of LaGrange county, the Geological Survey of 1873

reported the dense forests that had once covered over half the county were described as being preserved only as “oak openings” and a few small prairies (Cox, 1873). A state-level analysis by Evans et al., (2001) found that of the 85% of land in Indiana once covered by forests almost all of it had been cleared for agriculture and grazing after colonial settlement. Only 20% of those forests have regrown as of present. The result of the deforestation of the eastern United States from early settlers far extended beyond the boundaries of their communities. Evidence of a dust horizon, from wind erosion of soils can be seen in undisturbed peat lands in the eastern United States; possibly fertilizing these nutrient-poor ecosystems and altering plant communities (Ireland et al., 2014). In addition to the devastation of vegetation, numerous animal species such as bison, elk, the passenger pigeon, wild turkey, and white-tailed deer were extirpated before the 1900’s (Sieber and Munson, 1992; Jenkins, 2013). Although a vast period of Indiana’s land use history was occupied by Native Americans there was a significant impact to the geochemistry of Martin Lake caused by colonial settlers. This transition between Native American and colonial settlement and the effects it had are the focus of this study.

1.3 Chapter 1 References

Bird, B. W., Wilson, J. J., Gilhooly III, W. P., Steinman, B. A., & Stamps, L. (2017). Midcontinental Native American population dynamics and late Holocene hydroclimate extremes. Scientific Reports, 7, 41628.

Carman, S. F. (2013). Indiana forest management history and practices.

Cochran, D. R. (2004). Culture History of Indiana. Ball State University, Muncie, IN.

Cox, E.T. (Ed.) (1874). Fifth Annual Report of the Geological Survey of Indiana. Indianapolis, IN: Sentinel Company, Printers.

Evans, T. P., Green, G. M., & Carlson, L. A. (2001). Multi-scale analysis of landcover composition and landscape management of public and private lands in Indiana. In GIS and remote sensing applications in biogeography and ecology (pp. 271-287). Springer, Boston, MA.

Ireland, A. W., Clifford, M. J., & Booth, R. K. (2014). Widespread dust deposition on North American peatlands coincident with European land-clearance. Vegetation history and archaeobotany, 23(6), 693-700.

Jenkins, M. A. (2013). The history of human disturbance in forest ecosystems of southern Indiana. In: Swihart, Robert K.; Saunders, Michael R.; Kalb, Rebecca A.; Haulton, G. Scott; Michler, Charles H., eds. 2013. The Hardwood Ecosystem Experiment: a framework for studying responses to forest management. Gen. Tech. Rep. NRS-P-108. Newtown Square, PA: US Department of Agriculture, Forest Service, Northern Research Station: 2-11., 2-11.

Sieber, E., & Munson, C. A. (1992). Looking at history: Indiana's Hoosier National Forest region, 1600 to 1950. US Dept. of Agriculture, Forest Service.

Thornton, R. (2000). Population history of native North Americans. A population history of North America, 9-50.

Wobst, H. M. (1976). Locational relationship in Paleolithic society. Journal of Human Evolution London, 5(1), 49-58.

CHAPTER 2

2.1 Introduction

2.1.1 Knowledge Gaps

This thesis addresses two related problems in limnology: (**1**) the effects that deforestation has on the redox conditions of a lake, and (**2**) the difficulties in which redox conditions are typically deduced in limnological studies. Deforestation is the anthropogenic clearing of trees to make the land available for other uses. This along with its compliments, reforestation (replanting trees in a once forested area) and afforestation (planting trees in a barren land in order to create a forest), are all important and well-studied topics that have been researched across multiple disciplines. The human alteration of the landscape has profound impacts socio-politically, in terms of "environmental refugees" (Myers, 2002), economically (Angelsen and Kaimowitz, 1999; Barbier and Burgess, 2001), climatically (Bonan, 2008), and ecologically, as it pertains to habitat loss (Rask et al., 1993; France, 1997; Lorion and Kennedy, 2009). Lakes are a great recorder of aquatic-terrestrial linkages on both local scales (e.g. land-use changes) and global scales (e.g. climate change); they have become the sentinels of environmental change (Williamson et al., 2008; Adrian et al., 2009). Lakes contain important archives for understanding environmental changes because (**1**) they respond directly to climate and environmental change; (**2**) integrate responses over long time periods, which filters out the complexities of background noise; (**3**) are distributed worldwide allowing for the study and comparison of many different environments; (**4**) and contain high-resolution archives that are sensitive records of human activity because human population centers tend to develop around lakes (Adrian et al., 2009).

Land-use change critically alters lake environments and can have profound and lasting effects on oxygen availability that radically alter lacustrine ecology. For example, nutrient loading from sewage and agricultural practices can lead to eutrophication, increased sedimentation, and increased dissolved organics that can decrease light penetration that changes the thermal structure of the lake (Solomon et al., 2015).

Although there are studies which report changes in temperature and oxygen stratification (Rask et al., 1993; France, 1997; Andrew et al., 2008) as a result of deforestation and its compliments, these studies do not directly relate changes in forest management to the changes in past redox conditions (known as paleoredox) preserved in lake sediments. Exploration of redox environments gives us an inorganic geochemical window into the past lake conditions, in which meaningful relationships between oxygen conditions can be correlated to terrestrial land changes through other common lacustrine proxies (i.e. $\delta^{13}C$, $\delta^{15}N$, TC, C/N, etc.). A novel approach that uses the redox reactivity of iron (Fe) to track redox conditions in marine sediments (Raiswell et al., 2018), has the potential to be an important tool to use in conjunction with other sediment markers of deforestation, such as increased sedimentation.

Refining proxies that better constrain paleoredox conditions in lakes has significant potential for understanding the history of a lake regarding the interactions between the hydrosphere, biosphere, geosphere, and the focus of this study: *the anthroposphere*. A variety of approaches are used to determine different depositional redox environments including paleoecological methods, micropaleontological techniques, organic geochemical indictors, carbon-sulfur relationships, and isotopic and mineralogical data (Raiswell et al., 1988). These methods all have disadvantages due to preservation or availability issues, sample size and time limitations, or ambiguous results (Raiswell et al., 1988). Moreover, paleoecological visual-based cues, such as bioturbation and fine laminations (Raiswell et al., 1988), are unable to distinguish more specific redox conditions like water columns containing dissolved iron (ferruginous) or sulfide (euxinic). Ferruginous and euxinic conditions are physiological stressors to aquatic fauna. Dissolved sulfide is toxic to all animal life and its effects on invertebrates that live in the sediment and fish have been extensively studied (Oseid et al., 1974; Abel et al., 1987).

Iron geochemistry has widely been used as the key approach to assess local oxygen conditions in ancient marine environments. The Fe-based redox proxies are based on the observation that iron mineral phases that are reactive towards hydrogen sulfide (iron in oxides, carbonates, magnetite, pyrite, and acid volatile sulfur) on short diagenetic timeframes (Poulton and Canfield, 2004) are enriched relative to the total Fe

pool in sediments deposited within anoxic waters (Raiswell et al., 2018). These Fe-based proxies too have limitations, but in combination with other methods, such as sedimentological and paleoecological examination, isotope work, or trace metal geochemistry, they can provide a convincing and more nuanced view of redox conditions in aquatic settings (Raiswell et al., 2018).

As calibrated from empirical data, the distribution of iron in marine sediments and Paleozoic sedimentary rocks can be used to determine whether the bottom waters were oxic or anoxic and ferruginous or euxinic (Figure 1). The ratio of highly reactive iron to total iron (Fe_{HR}/Fe_T) can be used to determine oxic verses anoxic conditions; values below 0.22 are considered oxic and those above 0.38 anoxic. In sediments that were deposited in anoxic bottom water, ferruginous conditions can be distinguished from euxinic ones by considering the extent of pyritization of the highly reactive iron pool (Fe_{pyr}/Fe_{HR}) (Poulton and Canfield, 2011). Best practice thresholds suggest that Fe_{pyr}/Fe_{HR} values below 0.7 are considered to be ferruginous, while higher values denote euxinia (Raiswell et al., 2018). These Fe-based proxies for determining marine oxygen conditions have yet to be widely applied to lacustrine environments. Relative to marine settings, lacustrine environments can experience extreme fluctuations in oxygen and redox condition that occur on seasonal or decadal time scales. Likewise, lakes can undergo broad changes in

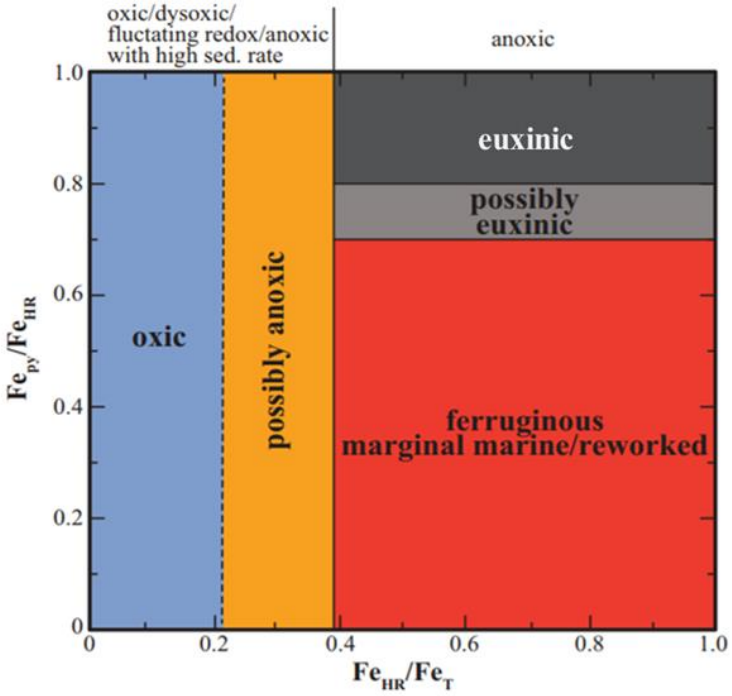

Figure 1: Diagnostic fields of Fe_{pyr}/Fe_{HR} and Fe_{HR}/Fe_T based on empirical thresholds for marine sediments. Solid lines are the recommended values and the dashed line is a suggested boundary for ancient sediment (Modified from Raiswell et al., 2018).

pH, water balance, and dissolved ion chemistry on residence times that are much faster than the ocean. A recent application of this proxy was used in Lake Huron (Rico and Sheldon, 2019). Here we propose the implementation of Fe-based proxies to study the development history of Martin Lake, Indiana.

2.2 Hypothesis

Meromictic (permanently stratified) and monomictic (seasonally mixed) lakes preserve sedimentary and geochemical records of past environmental conditions. Within lakes that stratify, water column anoxia prevents the establishment of benthic fauna, resulting in a lack of bioturbation and allowing the preservation of laminated sediments (Hughen et al., 1999). A laminated sequence is a powerful interpretive tool because it provides a high-resolution time scale for determining rates and timing of lacustrine processes, biological succession, and climate change (Anderson et al., 1985). New research focusing on geochemical proxies will help bridge the gap between forestry management and its effect on the geochemical processes within the lake**. I hypothesize that after colonial settlement, when the area was deforested, climate conditions took an auxiliary roll to the anthropogenic induced conditions, thereby pushing the once oxic Martin Lake to anoxic (and likely ferruginous) conditions.** This hypothesis presents the idea that under the two extreme conditions in land coverage, forested and clear cut, there will be notable differences in important geochemical markers that can reveal details of past redox conditions. During the time before colonial settlement, when LaGrange County was forested, we expect to find evidence for prolonged oxic conditions, due to weaker thermal stratification during the LIA, because of shorter warm-season periods during this climatic interval. Under these conditions controlled by climate, the highly reactive iron ratios preserved in the sediment should show signs of prolonged oxic conditions. In contrast, during colonial colonization of the area around the 1800's the forest surrounding Martin Lake was harvested. At this time, it is expected

that the lake would have become anoxic due to the physical and chemical effects of deforestation. The presence of anoxia and possible ferruginous or euxinic conditions can be indicated by Fe-based paleoredox proxies (Lyons and Severmann, 2006; Poulton and Canfield, 2011; Reinhard et al., 2013). This proxy is discussed in detail later (see Reactive Iron Ratios; 2.3.4.1). In short, it is expected that during times of prolonged anoxia the ratio of highly reactive iron to total iron will be higher than during periods of oxygenated waters.

2.3 Background

2.3.1 Study Site

Martin Lake is a monomictic lake in LaGrange County, Indiana. It is part of an interconnected chain of lakes that include Oliver, Olin, Martin, and Smith Hole. The first three are marl lakes, exhibiting highly calcareous waters (Wetzel, 1966). During the warm season, autochthonous calcium carbonate (calcite) is precipitated in the upper portion of the water column of Martin Lake. Under anoxic conditions, this accumulates as rhythmic mm-scale couplets of detrital/organic matter and authigenic calcite laminae (Bird et al., 2017). Within the core Marin Lake contains laminated sediments below 71 cm. The basin of Martin Lake has the classic uniform morphology of a kettle lake, having a steep gradient

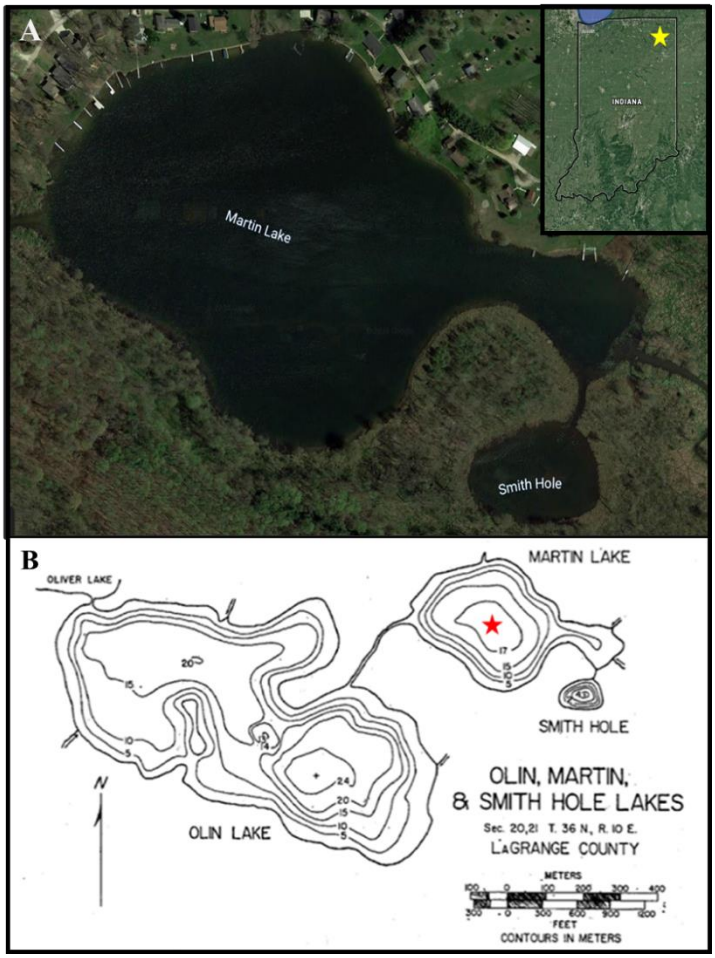

Figure 2: Location and hydrology of Martin Lake. **A**) Location of Martin Lake, in LaGrange County, Indiana. **B**) Hydrographic map of Martin Lake, and the two lakes directly connected to it (Wetzel, 1973). The red star represents the sampling site.

from the marl shelves to a relatively flat 17 m deep bottom (Wetzel, 1973). The lake is fed by two minor ephemeral streams and the inlet from Smith Hole, to the South, in addition to contributions from near surface groundwater (J.F. New, 2009). Martin Lake has a constant outflow through a western outlet into the northeastern end of Olin Lake (Wetzel, 1973), creating a hydrologically open system with a short mean residence time of 110 days (J.F. New, 2009). Despite open conditions, Martin Lake remains stratified throughout the year, turning over once in late December or early January (Bird et al., 2017).

2.3.1.1 Historical Record of Martin Lake

A 2100-year-long multi-proxy hydroclimate record for the Midwest region was developed by Bird et al. (2017) using Martin Lake as the study site. Regional and local changes in overall precipitation, rain events, and warm-season duration were correlated to the Pacific North American pattern (PNA). The PNA is the most prominent contribution to Northern Hemisphere climate variability (Leathers et al., 1991; Rogers and Coleman, 2003). The positive phase of the PNA pattern is associated with strong ridge and trough atmospheric circulation that brings moisture and airmasses from the northwest into the Midwest causing increased winter precipitation and decreased summer precipitation. The negative PNA phase accompanies more zonal atmospheric flow with clockwise atmospheric circulation, steering airmasses and moisture from the Gulf of Mexico into the Midwest, bringing more summer precipitation (Leathers et al., 1991).

During the Medieval Climate Anomaly (MCA; 950-1250 CE), wet warm-season (and dry cold-season) midcontinental climate conditions reflect negative PNA-like conditions (Bird et al., 2017). Dryer warm-season conditions in the Little Ice Age (LIA; 1250-1830 CE) characterized the midcontinent, reflecting a positive PNA-like condition (Bird et al., 2017). From Martin Lake, in particular, oxygen and carbon isotopes in carbonates $\delta^{18}O_{carb}$ and $\delta^{13}C_{carb}$ were used as proxies for source of midwestern precipitation and warm-season duration, respectively. The amount of siliciclastic input (measured as % lithics) was also used as a proxy for occurrence of warm-season rainstorm events. The deforestation of LaGrange County is marked in the sediment

record of Martin Lake as a large influx of % lithics (Figure 3B) (Bird et al., 2017). The decrease in water availability in the Midwest region during the late Holocene is corroborated by the anthropologic record of the Native American population, described in Chapter 1.

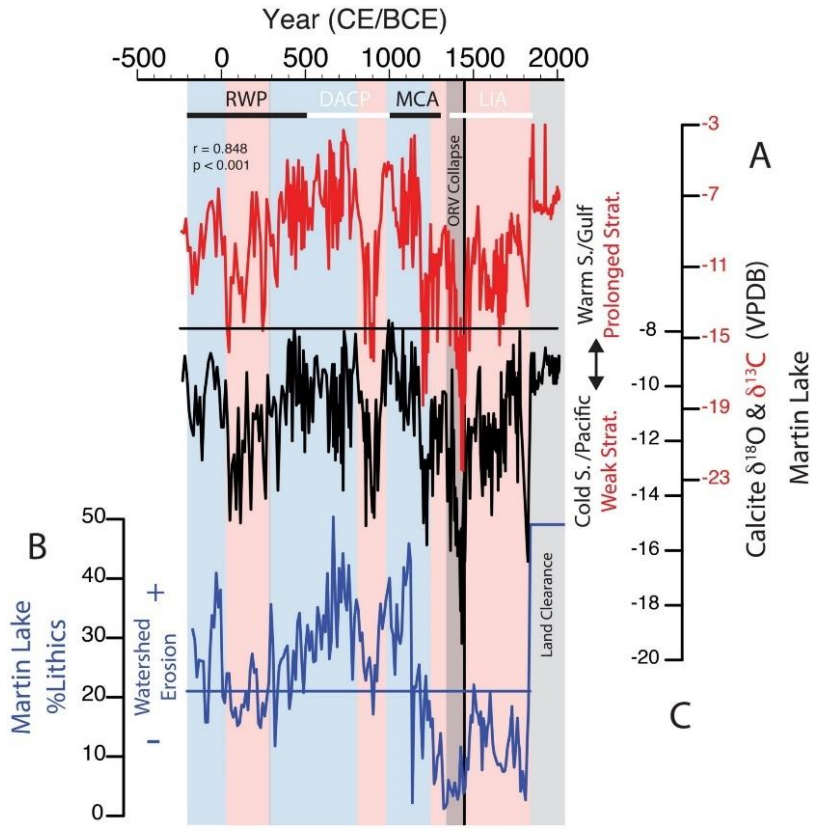

Figure 3: Modified summary of Martin Lake data from Bird et al. (2017). **A**) $\delta^{13}C$ in red, **B**) % lithics, **C**) $\delta^{18}O_{cal}$ in black. The x-axis displays the time period: Roman Warm Period (RWP), Dark Ages Cold Period (DACP), Medieval Climate Anomaly (MCA), and the Little Ice Age (LIA) along with their corresponding years either CE or BCE. Land Clearance in the modern at about 1840 CE is indicated by the light grey bar.

2.3.2 Seasonal Turnover and Stratification

Thermal stratification in lakes is an important phenomenon in temperate regions, which experience large contrasts in seasonal temperature and precipitation. At the end of winter, when any remaining ice has melted, the water at all depths is near the maximum density. Slight changes in temperature above and below this can cause larger shifts in

density, causing a sharp decrease in thermal resistance to mixing, thus allowing only small amounts of wind energy to completely mix the water column. Warm monomictic lakes, like Martin Lake, only experience spring turnover (Wetzel, 1973). As spring progresses, the surface waters of lakes of moderate depth (typically >6 m) are heated faster than the heat can be distributed through mixing. As the surface waters warm and become less dense, the relative resistance to mixing increases to a point were circulation ceases. At the onset of thermal stratification, the water column is divided into three regions, which are resistant to mixing. The colder bottom waters (the hypolimnion) remain relatively undisturbed for the duration of stratification. The surface water, or epilimnion, essentially floats on the hypolimnion and is fairly turbulent and circulates frequently. The layer between the epilimnion and hypolimnion is termed the metalimnion and contains the sharp thermal gradient (thermocline) between warm epilimnion and cold hypolimnion waters. There are many variables that control the ways and times that lakes stratify or not. Over longer time scales, climate can become an important inducer of changes in typical stratification regimes (Wuebbles and Hayhoe, 2003; Ficker et al., 2017), but over decadal time scales, changes in air temperature are not a significant driver of changes in thermal properties (Andrew et al., 2008).

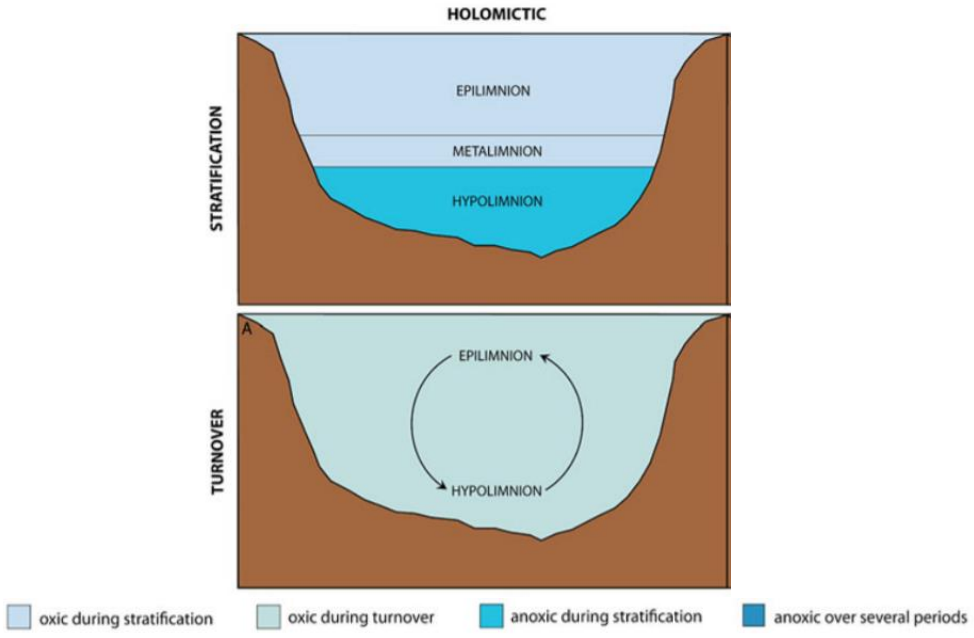

Figure 4: Patterns of stratification and turnover in holomictic and meromictic lakes (modified from Koeksoy et al., 2016).

Wind and underwater light attenuation are important drivers for whole lake turnover and thermal stability (Andrew et al., 2008) that are sensitive to catchment forest coverage. Conditions are expected to change based on the surface roughness of the landscape surrounding the lake (such as the presence or lack of trees) and light penetration impeded by an increase in sedimentation and dissolved organic matter (DOM), usually measured as dissolved organic carbon (DOC). Terrestrial DOM is made up of a suite of substances that originate from the tissues of terrestrial plants that have been modified within the soil environment and washed into the lake by runoff or groundwater (Nebbioso and Piccolo, 2013). Deforested lakes typically have higher DOC content, and thus lower water clarity, caused from increased runoff due to a lack of trees (France, 1997; Rosenmeier et al., 2002). Higher DOC concentrations in more turbid waters promotes greater light attenuation with depth. These conditions enhance the absorption of solar radiation which heats the upper water column, causing thermocline to move towards the lake surface (Solomon et al., 2015). Surface-weighted heat distribution causes thermal stratification to occur closer to the surface, which results in a more stable whole lake stratification (Read and Rose, 2013). The reduction of littoral shading due to deforestation had no effect on water temperatures or thermal stratification; instead, average water temperatures are likely related to regional air temperatures (Steedman et al., 1998).

2.3.3 Carbon Isotope Fractionation in Lakes

The new research into lake redox proxies presented here can be connected to forestry management, based on the carbon isotope composition of authigenic carbonate ($\delta^{13}C_{carb}$) and % lithics determined in a previous study by Bird et al. (2017), in addition to the $\delta^{13}C$ of organic carbon within the sediment ($\delta^{13}C_{org}$). The inorganic carbon isotope composition of dissolved HCO_3^- (Dissolved Inorganic Carbon; DIC), is a commonly used proxy in lacustrine paleoclimate studies. Carbon isotopes are fractionated during different transitions in the carbon cycle and become incorporated into authigenic and biogenic carbonates. In general, there are three predominant processes that control the carbon isotope composition of the DIC: the isotope composition of inflowing waters, CO_2

exchange between atmosphere and lake water, and photosynthesis/respiration within the lake (Leng and Marshall, 2004).

2.3.3.1 $\delta^{13}C_{DIC}$ Contribution of Surface and Groundwater

Martin Lake is fed by an inflow of convergent ephemeral streams and near surface groundwater (Bird et al., 2017). Calcite precipitated from groundwater and river water typically has values between -10 and -15‰ (Andrews et al., 1993). A significant portion of the carbon found in groundwater comes from plant respiration and production of CO_2 in soils. Terrestrial derived C3 plant matter (e.g., commonly trees and shrubs) has a $\delta^{13}C$ value between -32 and -20‰. Higher $\delta^{13}C$ values, in the range of -17 to -9‰, do occur, but are restricted to C4 plants, which are most commonly grasses, but also include common agricultural crops such as corn (Meyers, 1994). CO_2 production, via the decay of terrestrial organic matter, within the soil causes isotopically light $^{12}CO_2$ to enter soil waters and shallow groundwater (Leng and Marshall, 2004). At a pH of approximately 7 to 10, the dominant carbon species is HCO_3^- (Leng and Marshall, 2004), which, when in equilibrium with CO_2 gas, has $\delta^{13}C$ values of about 10‰ higher than CO_2 (Romanek et al., 1992). This means that HCO_3^- derived from soil CO_2 with a $\delta^{13}C$ of C3 terrestrial plant, should have $\delta^{13}C$ values roughly between -22 and -10‰, which is within the range of measured groundwater. Much higher $\delta^{13}C$ (-3 to +3‰) in groundwater can occur in karstic regions (Andrews et al., 1997), which is not of concern in this study of Martin Lake.

CO_2 exchange can also affect the $\delta^{13}C$ values for DIC in lakes. Often, carbonates in lakes are precipitated with high $\delta^{13}C$ values that are covariant with high $\delta^{18}O_{carb}$ values, this is true of Martin Lake (Figure 3). In hydraulically closed systems, high values of $\delta^{13}C$ and $\delta^{18}O_{carb}$ reflect different degrees of equilibration of the DIC with atmospheric CO_2 and preferential evaporative loss of the ^{16}O (Leng and Marshall, 2004). Martin Lake is an open system, so the effects of CO_2 exchange are less important. In Martin Lake, $\delta^{18}O_{carb}$ has been shown to reflect the regional precipitation for Indiana and is not influenced by evaporation (Bird et al., 2017).

2.3.3.2 Photosynthesis and Respiration within the Lake

Biological productivity within lakes is a driving force for changes in the DIC pool, and its isotopic composition is controlled mainly by the preferential uptake of ^{12}C during photosynthesis in the water column (Leng and Marshall, 2004). Preferential uptake of ^{12}C during periods of enhanced productivity causes the carbon pool to become enriched in ^{13}C, consequently increasing $\delta^{13}C_{DIC}$; these changes can be seasonal and are often caused by summer stratification in the water column (Leng and Marshall, 2004). Increased productivity in the epilimnion, due to a new supply of nutrients from lake overturn, may lead to significant differences in $\delta^{13}C$ of dissolved inorganic carbon (Leng and Marshall, 2004). Permanent stratification of the water column can cause even larger changes in $\delta^{13}C$ of authigenic carbonates (Leng and Marshall, 2004). Before prolonged stratification, the lake remains well mixed and ^{13}C values for authigenic calcite remain relatively high. At the onset of permanent hypolimnion anoxia, the rate of organic matter oxidation slows, thus causing even more positive $\delta^{13}C$ values, since there is no longer ^{12}C-enriched dissolved inorganic carbon coming from the decay of organic matter (Leng and Marshall, 2004).

2.3.3.3 Carbon Isotope Signatures of Organic Matter

Organic matter in lake sediments primarily originates from the particulate detritus of plants and algae, with only a small fraction coming from animals. Extensive early diagenetic losses of organic matter do not appear to alter the ability to categorize organic matter sources using bulk identification (Meyers, 1994; Meyers and Lallier-Verges, 1998). Plants and algae generally incorporate the lighter ^{12}C, which leads to an enrichment of ^{12}C over ^{13}C in many types of organic matter; C3 and C4 plants leave distinct isotope signatures because of these fractionations. Most photosynthetic plants incorporate carbon into organic matter using the C3 Calvin pathway, which preferentially takes up ^{12}C. C3 plants, which make up 85% of land plants (e.g. most trees, shrubs, and winter grasses) are more isotopically depleted in ^{13}C relative to C4 plants. Some plants use the C4 Hatch-Slack pathway, which is more efficient than photorespiration.

Photorespiration is an inefficient pathway within the Calvin cycle that occurs when the enzyme rubisco binds to oxygen instead of carbon dioxide. C4 plants have $\delta^{13}C$ values ranging from -17 to -9‰, whereas C3 plants have values between -32 and -20‰ (Meyers, 1994). Alternations between C3 and C4 watershed plants accompany changes in climate transitions, precipitation, and land-plant type, and are apparent in $\delta^{13}C$ values of sedimentary organic matter (Meyers and Lallier-Verges, 1998). Freshwater algae utilize dissolved CO_2, which is usually at equilibrium with atmospheric CO_2. This means that the $\delta^{13}C$ composition of lake-derived organic matter, such as algae, is almost isotopically indistinguishable from organic matter from the surrounding watershed (Meyers, 1994). C/N ratios can be used to further distinguish algae from C3 land plants, as they have much different ratios, 0-10 and 25-75, respectively (Meyers, 1994).

2.3.4 Iron and Iron-Sulfur Minerals in Lakes

The carbonate isotopes provide a record of water column thermal stratification ($\delta^{13}C_{carb}$) and water source ($\delta^{18}O_{carb}$); however, neither indicate the extent of oxygenation in the bottom waters. Oxygen deficiency in response to climatic change has become a pervasive and prevalent problem in lakes and the ocean (Golosov et al., 2012). We provide here an approach to applying an iron redox proxy developed for marine sediments to better constrain past oxygen availability in lacustrine archives. Microbial decay of organic matter within sediments uses a suite of terminal electron acceptors including sulfate (Konhauser et al., 2011). Although sulfate concentrations are generally low in North American temperate lakes (Cook and Kelly, 1989), the microbial utilization of sulfur and subsequent reactions with available iron produces an assemblage of iron minerals that can be used to reconstruct water column redox conditions (Raiswell et al., 2018). Hydrogen sulfide, produced by sulfate reducing bacteria during the mineralization of organic matter, reacts with Fe minerals to form FeS (acid volatile sulfide; AVS), which then either reacts directly with H_2S or with partially oxidized S species (e.g., S_8 and polysulfides) to form pyrite (FeS_2), in the absence of oxygen (Raiswell et al., 2018). A portion of the sulfur is in the form of AVS and the concentration of this iron sulfide mineral reflects a balance between iron availability, sulfide production, and oxidation

(Leonard et al., 1993). In modern sediment, Fe-AVS is also an important portion of the highly reactive iron pool, which is used in the Fe-based redox proxies. Higher AVS concentrations are consistent with organic-rich, anoxic sediment, with lower concentrations found in oxic sediments that contain low amounts of organic carbon (Burton et al., 2007). The extent of pyrite formation is thought to be limited by the amount of microbial sulfide produced, the availability of reactive Fe minerals, or the lack of organic carbon (Raiswell and Canfield, 1998; Raiswell et al., 2018). Thus, the amount of pyrite in the sediment can be a relative measure of the availability of those three main components, in addition to being an important part of the Fe_{HR} pool used in the Fe-based proxies.

2.3.4.1 Reactive Iron Ratios

Iron redox proxies relate the amount of iron that is highly reactive (Fe_{HR}) to sulfide relative to the total amount of iron (Fe_T) in the sediment and the portion of that reactive iron that has become pyrite (Fe_{pyr}). These two ratios (Fe_{HR}/Fe_T; Fe_{pyr}/Fe_{HR}), in marine settings, when used in conjunction with other proxies or sedimentological context, have been shown to be relatively straightforward and robust indicators of bottom water redox (Lyons and Severmann, 2006). Modern oxic sediments deposited in a wide range of depositional environments have been shown to have a Fe_{HR}/Fe_T ratio less than 0.38, which defines the modern siliciclastic baseline (Raiswell and Canfield, 1998). Under anoxic conditions, iron is remobilized through reductive dissolution (Lyons and Severmann, 2006) and authigenically enriched relative to detrital inputs resulting in Fe_{HR}/Fe_T values above this threshold (Poulton and Canfield, 2011). Empirical calibration of this ratio shows natural variation such that values between 0.22 and 0.38 may either be

oxic or anoxic but should be considered in conjunction with sedimentation rate and other proxies (Poulton and Canfield, 2011). In sediments that were deposited in an anoxic environment, ferruginous conditions can be distinguished from euxinic ones by considering the extent of pyritization of the highly reactive iron pool (Fe_{pyr}/Fe_{HR}) (Poulton and Canfield, 2011). An anoxic system that has a relatively minor fraction of Fe_{HR} converted to pyrite is indicative of a ferruginous environment in which the reactive Fe supply was greater than the titrating capacity of H_2S, meaning that no excess H_2S accumulates in the water column (Reinhard et al., 2013). Best practice thresholds suggest that Fe_{pyr}/Fe_{HR} values below 0.7 are considered to be ferruginous, while higher values denote euxinia (Raiswell et al., 2018).

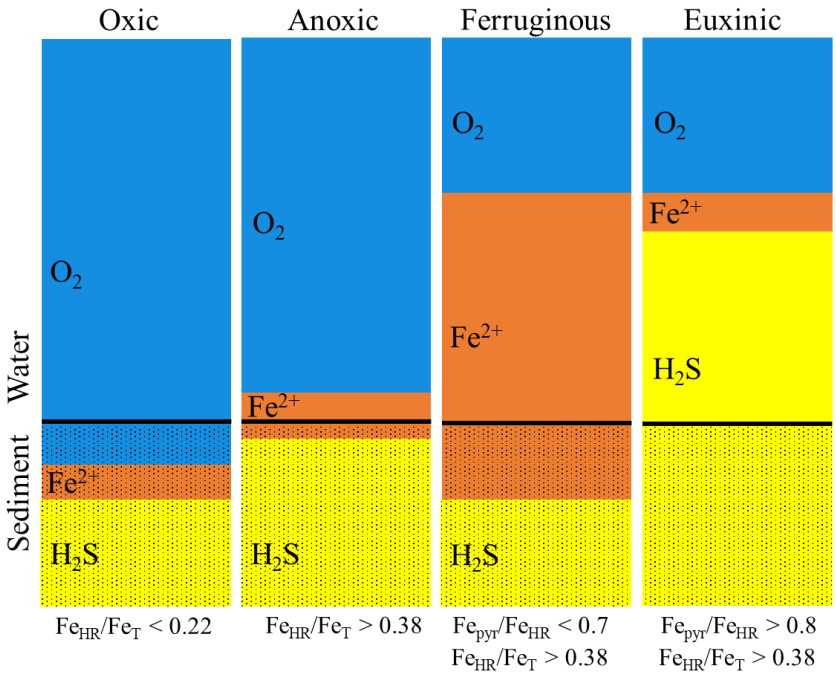

Figure 5: Best practice thresholds for Fe_{pyr}/Fe_{HR} and Fe_{HR}/Fe_T ratios, and their implications in water column redox states. This simplified water column aims to show the relative amounts of iron, hydrogen sulfide, and oxygen for each of the respective redox conditions that these Fe-based proxies shows. Modified from (Poulton and Canfield, 2005; Lyons and Severmann, 2006).

The two ratios and their respective threshold values are summarized in Figure 5, along with a simplified depiction of the water column chemistry of each redox scenario (oxic, anoxic, ferruginous, and euxinic). Because this proxy was developed for use in marine, sulfur-rich systems (relative to lacustrine) with deep shelf-to-basin transport (Raiswell and Canfield, 1998), its application to shallow lacustrine basins requires careful consideration. Relative to the average depth of the ocean, it becomes difficult to discern

whether this proxy demonstrates the redox chemistry of the entire water column, the redox-cline above the sediment-water interface, or that of the porewater in these shallow basin systems (Rico and Sheldon, 2019). Based on new research by Rico and Sheldon (2019) in Lake Huron, it has been suggested that Fe redox proxies likely provide a snapshot of the water column chemistry and are not necessarily able to project the expanse of anoxic redox conditions (i.e. the depth of the chemocline). In Martin Lake, it is expected that both extremes (prolonged anoxic or oxic waters) will be indicated by these Fe-based proxies. Pre-settlement, during the LIA, when Martin Lake was weakly thermally stratified, it is expected that the record will show prolonged oxic conditions. After the land was anthropogenically altered through deforestation, it is expected that Martin Lake switched to being primarily anoxic or even ferruginous. This likely can be attributed to several factors such as an increase in sulfide due to a loss of sulfate retention in soils (Nodvin et al., 1988), longer periods of lake stratification, and increased sedimentation.

2.4 Methods

2.4.1 Core Collection

On May 23rd, 2018 a 1 m push core ("Martin Lake Core- Henke- 2018") was taken from the center of the deep basin (Figure 2A) of Martin Lake, in LaGrange County, Indiana; 89 cm of mud was collected from that core. Zorbitrol© Plus Superabsorbent Polymer (Ulster Scientific Incorporated, New Paltz, NY), a sodium polyacrylate powder, was added to the bottom water remaining at the top of the core to prevent mixing of the sediment-water interface. This powder can absorb several times its weight in water and allows for safe transportation of the core in a non-vertical position, by turning the bottom water collected into a thick gel. In addition to preserving the sediment–water interface, this method shows no detectable effects on measurements of total organic carbon or total nitrogen values in the sediment (Tomkins et al., 2007). The core was then stored at 4°C until it was split into an archive half and a working half. The core was sampled every 2 cm and put into 50 mL centrifuge tubes that were purged with nitrogen gas to prevent

oxidation of iron and sulfur. The samples were stored frozen at -4°C until extracted for iron and sulfur. Splits for other measurements such as TC, TIC, TS, $\delta^{13}C$, and $\delta^{15}N$, were taken from the thawed portions of the mud within the 50 mL centrifuge tubes. These splits were portioned onto weigh boats and dried via a drying oven before use.

2.4.2 Magnetic Susceptibility

Magnetic susceptibility was measured at 0.5 cm intervals on the archive half of the core using a Bartington MS2 Magnetic Susceptibility Meter (Bartington Instruments Ltd, UK) attached to a GeoTek MultiSensor Core Logger (Geotek Ltd, UK). The archived core was stored under refrigeration at 4°C and was allowed to come to room temperature before magnetic susceptibility was recorded.

2.4.3 Bulk Compositions

Total carbon (TC) and total sulfur (TS) were analyzed from approximately 0.1 g of dry powdered sediment by combustion on an Eltra CS580 carbon sulfur analyzer (Eltra, Germany). Samples are corrected to both a carbon and sulfur standard: Buffalo River sediment (RM 8704, 3.351% C) and Coal (B2302, 0.73 ± 0.02 % S). Bulk inorganic carbon (TIC) of approximately 200 mg of dry sample was measured by acidification on the Eltra. The sample was moistened with 18 ΩH_2O and heated to 250°C. While stirring at 800 rev/min, using a stir bar, 6 mL of 50% phosphoric acid was added to digest the sample. A sample of calcium carbonate (AR-4013, 2.81 ± 0.05% C) was used as calibration. Total organic carbon (TOC) was found by subtracting TIC from TC. Similarly, TS is used to determine TOS via the difference between TS and $S_{AVS} + S_{pyr}$.

2.4.4 Stable Isotopes

The carbon isotope composition of organic matter ($\delta^{13}C_{org}$) was determined on dried sediments after carbonates were removed by acid fumigation. Samples were dried in a drying oven and 5-10 mg splits were weighed into 5x9 mm silver capsules. Each

sample capsule was placed into a 96 well plate. The plate was placed into a desiccator and 50 μL of 18 ΩH_2O was added to each sample. A 50 mL beaker of concentrated HCl was sealed with the samples in the desiccator and allowed to fume for 7-8 hrs. After fuming, the samples were placed in the fume hood and left to dry for approximately 24 hrs. Upon drying, the silver cups were placed into 5x9 mm tin cups and folded in order to increase the structural integrity and improve flash combustion in the elemental analyzer. The nitrogen isotope composition of total nitrogen ($\delta^{15}N$) in the sediment was determined on 10 mg splits of unacidified powdered sample to avoid any chemical alteration of the nitrogen isotope composition associated with acid extraction (e.g., Brodie et al., 2011). The sulfur isotope composition of AVS ($\delta^{34}S_{AVS}$) and pyrite ($\delta^{34}S_{CRS}$) was measured on acid extracts of the sediment that were preserved as silver sulfide (see method below).

Isotope compositions were analyzed by combustion on an EAIsolink (Thermo Fisher Scientific, USA) elemental analyzer coupled under continuous flow to a Delta V Plus (Thermo) stable isotope ratio mass spectrometer. Samples for carbon isotope analysis were corrected to reference materials USGS 40 ($\delta^{13}C$ = -26.39‰), Buffalo River Sediment ($\delta^{13}C$ = -19.86‰), and IAEA CH6 ($\delta^{13}C$ = -10.45‰). Samples analyzed for $\delta^{15}N$ were corrected to reference materials USGS 40 L-glutamic acid ($\delta^{15}N$ = -4.5‰), Buffalo River Sediment ($\delta^{15}N$ = +4.01‰), IAEA N1 ($\delta^{15}N$ = +0.4‰). Samples analyzed for $\delta^{34}S$ were corrected to reference materials IAEA S1 ($\delta^{34}S$ = -0.3‰), IAEA S2 ($\delta^{34}S$ = +22.62‰), IAEA S3 ($\delta^{34}S$ = -32.49‰). The stable isotope value of each sample was calculated according to:

$$\delta^{x}E = \left(\frac{R_{sample}}{R_{standard}} - 1\right) \times 1000‰$$

where each isotope value ($\delta^{x}E = \delta^{13}C$, $\delta^{15}N$, or $\delta^{34}S$) was reported as ‰ deviations of isotope ratio ($R = {}^{13}C/{}^{12}C$, ${}^{15}N/{}^{14}N$, or ${}^{34}S/{}^{32}S$) of the sample relative to the standard. Analytical precision was within ±0.1‰.

2.4.5 Acid Volatile Sulfur and Pyrite

Pyrite and AVS extractions were done on each sample in order to liberate the trapped sulfur and measure its concentration values. The chromium reduction method, outlined by Canfield et al. (1986), is implemented because it selectively extracts sulfur contained in reduced inorganic sulfur phases without liberating organic sulfur compounds or sulfates. AVS is the fraction of sulfide that is extractable by cold hydrochloric acid. It exists naturally in sediments mostly as iron monosulfide complexes (Leonard et al., 1993).

Sulfide was extracted from sediment samples in a glass extraction apparatus, which forms an air-tight seal with ground glass fittings. The digestion vessels contain luer-lock ports in which a 60 mL syringe was attached to inject the extraction solutions. Chilled water was continuously recirculated through condensing columns to condense acid vapor generated during the extraction. A section of tubing connects the top of the condenser to a sulfide trap, via a glass pipette that acts as a bubbling tube. The trap itself is a 50mL centrifuge tube, containing 25mL of 3% Zn-acetate and 10% NH_4OH. To start the sequential AVS-pyrite extraction, 1-2 mg of fresh, wet sample is weighed into the reaction vessel. The system is flushed with N_2 gas for 10 minutes to purge oxygen from the apparatus, and the flow rate was adjusted to bubble at a rate of 2-3 bubbles/sec. After leak checking the system, 20 mL of 6N HCl is injected into the reaction vessel and allowed to react for 45 minutes at room temperature.

After the AVS extraction, a new glass pipette and base trap containing 25 mL of 3% Zn-acetate- 10% NH_4OH was added to the extraction line. Approximately 3 mL of ethanol was added to the reaction vessels that contained the AVS extraction residues, to increase the solubility of elemental sulfur. A 60 mL plastic syringe was then filled with 40mL of a previously made $CrCl_2$ solution (1.0 M) and 20 mL of concentrated HCl; this reagent solution is then injected into the reaction vessel and the solution was boiled for 2 hours (Canfield et al., 1986). This method is specific to extracting reduced sulfur; sulfates and organic sulfur will remain in solution or in the residue within the extraction vessel.

After each extraction, a 3 mL split from each trap solution was stored at 4°C in cryogenic vials until analysis for sulfide concentrations using a spectrophotometer (DR

2800, Hach, USA). To the remaining trap solution, 3% $AgNO_3$- 10% NH_4OH was added to precipitate the sulfide as Ag_2S. This black precipitate was stored in the dark for at least one day to allow it to completely settle to the bottom of the centrifuge tube. The precipitant was then filtered through 0.22 µm filters (Whatman®) and rinsed with 18 ΩH_2O. The filter containing the precipitate was dried in an oven (40ºC), then weighed to calculate the sulfide concentration gravimetrically to confirm quantitative recovery. The samples were then homogenized using an agate mortar and pestle and stored in vials to be run for sulfur isotope composition.

2.4.6 Iron Extractions

The sequential iron extraction procedure isolates the reducible iron and manganese from carbonates (Fe_{carb}), oxides (Fe_{ox}), and magnetite (Fe_{mag}) from sediments (Poulton and Canfield, 2005). Dried sediment (0.4-0.9 g) was weighed into 15 mL centrifuge tubes and combined with 10 mL of sodium acetate (1 M), buffered with acetic acid to pH 4.5, vortexed, and reacted for 24 hours, while shaken at room temperature on a shaker table. Post reaction, the tubes were centrifuged for 5 minutes at 4000 rpm and an aliquot (1 mL) was preserved for measuring iron concentrations. The remaining solution in the tubes was decanted; 10 mL of sodium dithionite (50 g/L), buffered with acetic acid and sodium citrate to pH 4.8 was added and reacted for 2 hrs. Again, post reaction, the tubes were centrifuged, an aliquot was taken, and the remaining liquid decanted. Finally, 10 mL of ammonium oxalate (0.2 M)- oxalic acid (0.17 M), buffered with ammonium hydroxide to pH 3.2 was added and reacted for 6 hours. The tubes were centrifuged, and a final aliquot was taken. All three aliquots are diluted with 2% HNO_3 and the concentration of iron within each fraction was measured on an Atomic Absorption (AA) spectrophotometer (Perkin-Elmer, USA), using an Fe lamp with a wavelength of 248.3 (SCI Technology Inc., USA).

The total Fe_{HR} pool is comprised of mineral phases that are reactive to H_2S in short diagenetic timescales and those that have already reacted and are preserved as pyrite (Raiswell and Canfield, 1998). The amount of Fe_{HR} was calculated as the sum of

iron present as carbonates (Fe_{carb}), oxides (Fe_{ox}), magnetite (Fe_{mag}), pyrite (Fe_{pyr}), and AVS (Fe_{AVS}), where

$$Fe_{HR} = Fe_{carb} + Fe_{ox} + Fe_{mag} + Fe_{pyr} + Fe_{AVS}.$$

The amount of iron in pyrite and AVS was calculated based on the concentration of sulfur extracted by acid extraction, assuming a stoichiometry of FeS_2 and FeS.

Species	Reagent Step	Time	Phase	Minerals
FeCarb	1. Sodium acetate (1M) buffered with acetic acid to pH 4.5	24 h	Iron and manganese bound in carbonates	Iron carbonates
FeOx	2. Sodium dithionite (50 g/L) buffered with acetic acid and sodium citrate to pH 4.8	2 h	Iron and manganese oxides	Ferrihydrite, goethite, hematite
FeMag	3. Ammonium oxalate (0.2 M) and oxalic acid (0.17 M) buffered with ammonium hydroxide to pH 3.2	6 h	Magnetite	Magnetite

Table 1: Standard operating procedure for the sequential iron extraction for modern sediment.

2.4.6.1 Total Iron

Approximately 100-200 mg of sediment was weighed into microwave safe Teflon vessels and 10 mL of 6N HCl was added to extract total iron. The samples were heated for 30 minutes at 80-120 psi in a microwave digestion system (MDS 2000, CEM, USA). Total iron concentrations were analyzed on an ICP-OES (Optima 7000 DV, PerkinElmer, USA).

2.4.7 Bulk Density and Mass Accumulation Rate

Samples of the archive core were taken every 2 cm using a 1 cc sediment punch. These samples were placed in pre-weighed weigh boats and allowed to dry completely.

Post drying the samples were weighed again and the sedimentation rate and the mass accumulation rate were calculated using the formulas provided below.

$$Bulk\ Density\ (g/c^3) = \frac{Dry\ Weight\ (g)}{1\ cm^3}$$

$$Sedimentation\ Rate\ (cm/yr) = \frac{\Delta\ depth\ (cm)}{\Delta\ year}$$

$$Mass\ Accumulatio\ Rate\ (g/cm^2\ /yr) = Bulk\ Denisty * Sedimentation\ Rate$$

2.5 Results

2.5.1 Water Column

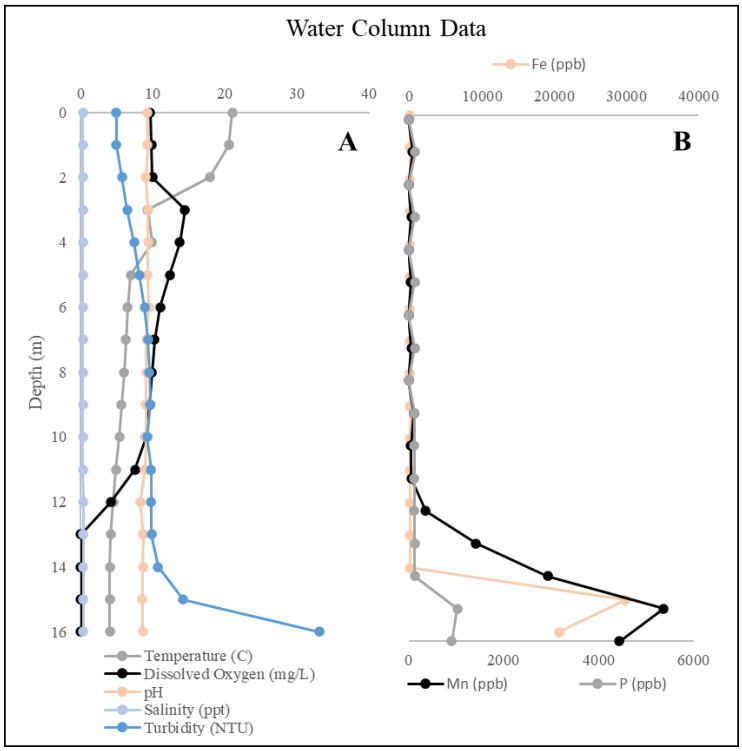

Figure 6: Water column data from Martin Lake. (**A**) Temperature (black), dissolved oxygen (grey), pH (orange), salinity (light blue), and turbidity (dark blue) were collected at the time of the core collection. **B**) Metals data Mn (black); P (grey); Fe (orange).

2.5.2 Age Model

An age model for the Martin Lake core was developed by correlating magnetic susceptibility patterns with those reported for a Martin Lake surface core by Bird et al., (2017) (Figure 7). In the previous study, accelerator mass spectrometry radiocarbon (^{14}C) ages were determined for samples comprised of charcoal fragments or terrestrial plant material at 63.5 cm and 16.5 cm core depth and were determined to have respective age dates of 1840 and 1980. The constructed age model for the Martin Lake core was based on these radiocarbon age dates and the sampling year (2013) for the surface sample (Figure 8A).

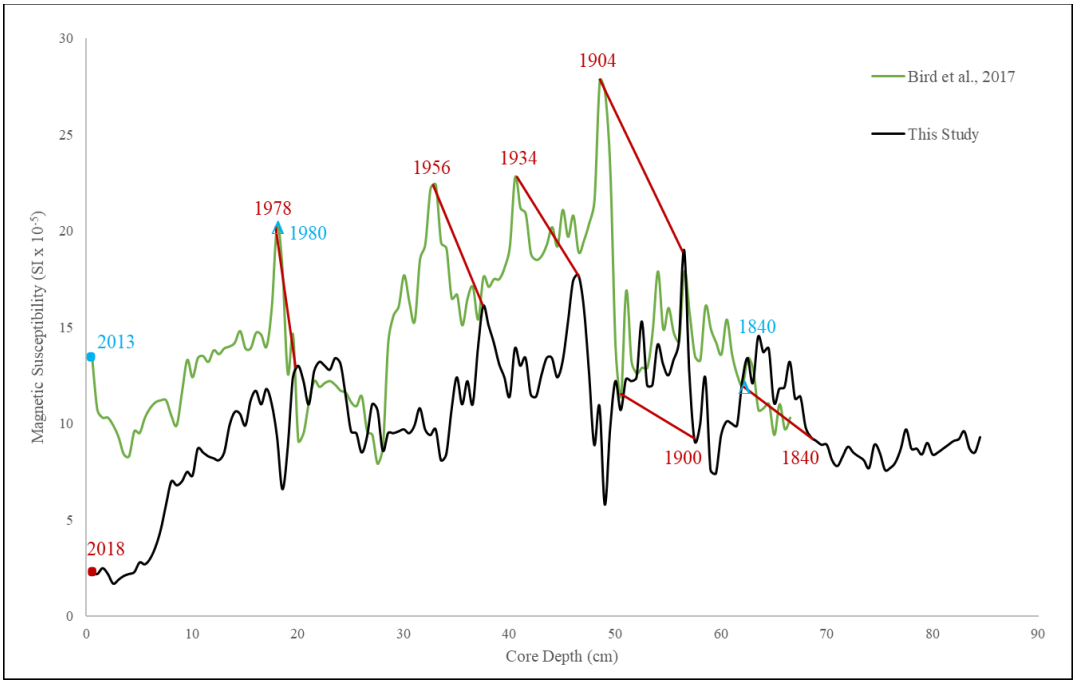

Figure 7: Comparison of magnetic susceptibility versus depth for both the Martin Lake (black line) core collected and the surface core from Bird et al., 2017 (green line). Red lines correlate distinct maxima in magnetic susceptibility. Blue triangles represent points where ^{14}C dates were collected in the study by Bird et al. (2017). Age dates are provided for clarity.

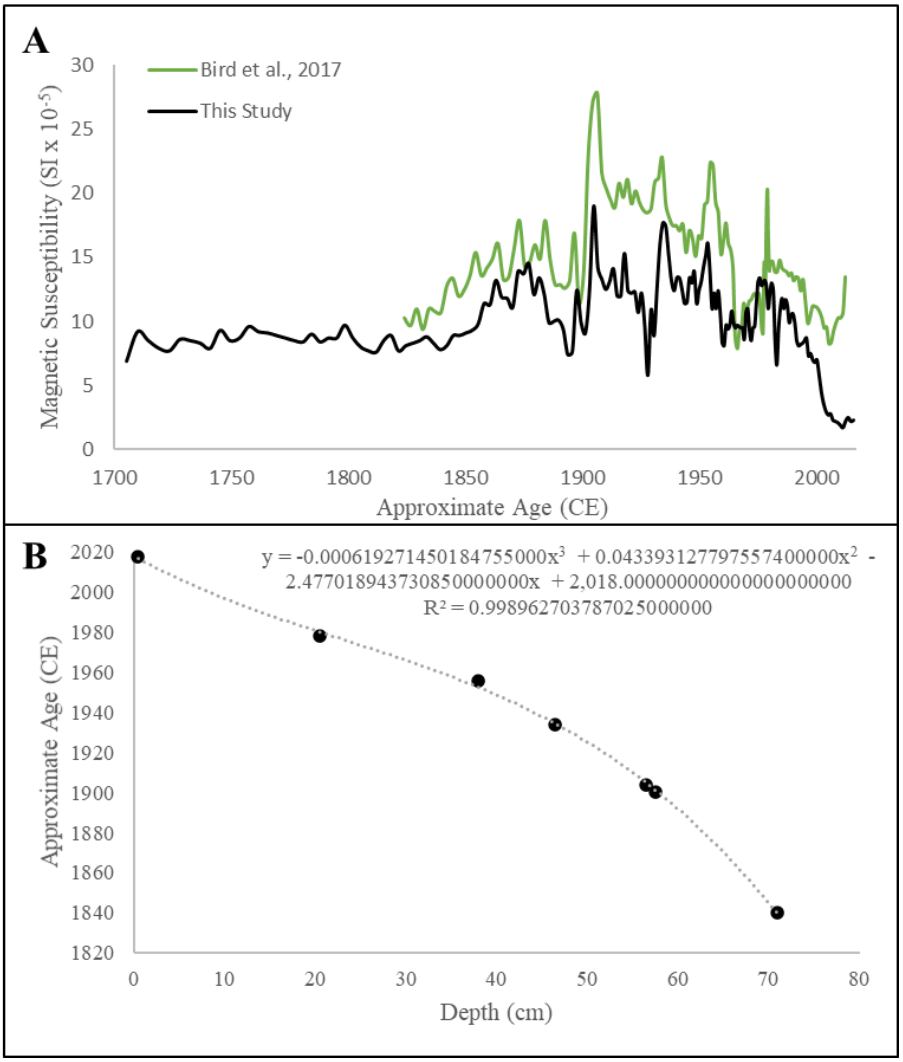

Figure 8: Age model graphs for Martin Lake (**A**) Comparison of the age model constructed for the Martin Lake core used in this study (black) and reference core from the Bird et al., 2017 (green). **B**) Regression curve calculated using 6 points, and the known point (2013) marking the top of the core, correlated from the Bird et al., 2017 magnetic susceptibility (Figure 7; dates in red).

2.5.3 Mass Accumulation Rate

Sedimentation and mass accumulation rates provide a lithological distinction between pre and post settlement that can subsequently be pared with the geochemical changes in the chemostratigraphy. Baseline values for mass accumulation rate and sedimentation rate are from 1700 to 1840 CE, during a time roughly 300 years after large Native American settlements up until the permanent settlement of colonist around 1840.

Values during this time were largely stable and comparatively much lower averaging 0.05 g/cm^2/yr and 0.10 g/cm/yr for mass accumulation rate and sedimentation rate respectively (Figure 9A & B). Baseline lithics data is more variable but remains on average low (Figure 9C). Post settlement both mass accumulation rate and sedimentation rate rapidly increased, averaging four times the pre-settlement baseline, and peaking in the late 1970s. Present day values although lower that at its peak remain much higher than baseline values. Lithic data increased even more rapidly, responding almost instantly to settlement. The % lithics throughout the post settlement era are much more variable than the mass accumulation and sedimentation rates and does not peak but remain overall higher than baseline values.

The error regarding this calculation could in future work be constrained with more accuracy by ^{210}Pb dating, but for this study we have confidence in our interpretations based on the age model given several factors. For one, ^{14}C age dated charcoal fragments reported by Bird et al., (2017) were isolated from the sediment transition between laminated and massive mud (i.e., the transition between pre and post settlement), and therefore that point is known with much certainty to be 1840. Using the magnetic susceptibility data, this point was then peak matched to the core from this study with great confidence (Figure 7). In addition, we can see lithologically that there is a change at this transition point; the sediment goes from even laminated layers to massive muds. This can be seen in the core image that accompanies Figures 10 and 11. We know that the transition happened at that depth and given the historical record and ^{14}C date we know the year in which that transition occurred. Furthermore, sedimentation appears to be uninterrupted throughout the lithological record, therefore the abrupt changes in geochemistry are reflection of evolving lake chemistry rather than any depositional hiatus or mass transport event.

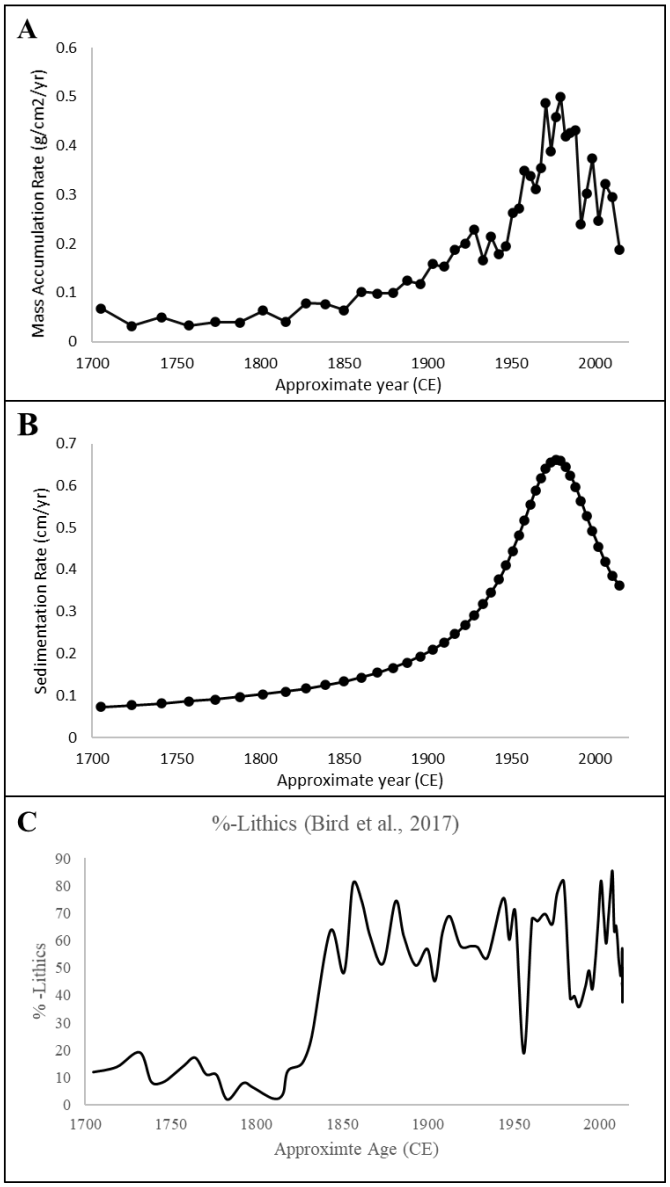

Figure 9: Sedimentation graphs for Martin Lake (**A**) Mass accumulation rate (g/cm^2/yr) of Martin Lake over time. (**B**) Sedimentation rate (cm/yr) over time. (**C**) % lithics collected from the 2017 Bird et. al study of Martin Lake over time.

2.5.4 Chemostratigraphy

The downcore variation in carbon, nitrogen, sulfur, and iron geochemistry is presented in Figure 10. The same elemental data have been normalized to mass accumulation rate in Figure 11 in order to resolve the dilution effects associated with the step increase in sedimentation observed in the upper half of the core. Within this portion

of the core, the sediments transitioned from laminated to massive mud. Isotopic values of $\delta^{13}C$, $\delta^{15}N$, $\delta^{34}S_{AVS}$, and $\delta^{34}S_{CRS}$, were not normalized to mass accumulation rate because these data were invariant relative to accumulation rate; isotopic data presented in Figures 10 and 11 are the same. Overall, pre-settlement values are less variable than after settlement. At the time of settlement there is a pronounced shift throughout all of these analytes, in which there are distinct changes in the average values pre and post settlement. These transitions occur at approximately 1840 in Figures 10 and 11.

Total inorganic carbon (Figure 11A) was relatively low throughout the core, averaging 1.8%. Prior to 1840, TIC average values were low at 0.7%, and then increased to much a higher average concentration of 2.2%. A similar increase was observed in TOC (A), averaging 0.6% before 1840 and 1.1% after. Within the last 50 years of the sediment record, TOC values on average have surpassed that of the pre-settlement baseline. The $\delta^{13}C$ values of organic carbon (B) averages -29.6‰ throughout the core. There was a significant increase in average values after 1840, transitioning from -30.7‰ to -29.2‰.

Nitrogen (C) throughout the core averaged 0.2%. Although these concentrations are generally low, there is a significant increase in average values from 0.1% to 0.2% after 1840. Like TOC, average N within the last 50 years of sedimentation has surpassed the pre-settlement average. Average $\delta^{15}N$ (C) within the lower part of the core was 2.6‰. These values abruptly increased to 4.5‰ after 1840. Values remained elevated throughout yet show a gradual up-core decrease in $\delta^{15}N$. The post 1840 $\delta^{15}N$ values average 6.2‰.

In comparison to the carbon and nitrogen data, the sulfur and iron data show a step change that transitioned to new baselines after 1840. The amount of TOS (D) is very low throughout the entire core (< 0.1%). Before 1840, the average TOS concentrations were 0.02%. There is effectively no TOS after 1840. For simplicity, the AVS and pyrite concentrations were combined together, as total reducible sulfide (TRS) (D). Sedimentary iron sulfides show a constant up-section increase throughout the core. Iron sulfides essentially account for all of the sedimentary sulfur pool in the upper, post-1840, portion of the core. The overall core average of TRS was 0.04%; the pre-1840 the average 0.005% increased by an order of magnitude to 0.05% after 1840.

The sulfur isotopic composition of AVS and CRS show identical patterns throughout the core; however, in all cases the $\delta^{34}S_{AVS}$ values are higher than $\delta^{34}S_{CRS}$ by an average of 2.6‰. Average $\delta^{34}S_{AVS}$ (E) throughout the core is -4.7 ‰ and $\delta^{34}S_{CRS}$ (E) is -6.7‰. The pre-1840 average was higher for both AVS and CRS at 1.8‰ and -0.8‰, respectively. After 1840, the average $\delta^{34}S_{AVS}$ and $\delta^{34}S_{CRS}$ decreased to -6.5‰ and -8.4‰, respectively. Pre-settlement $\delta^{34}S$ values are overall less variable and more positive. After 1840, the sedimentary sulfides decreased in isotopic composition with greater sample-to-sample variability. Within the last 50 years values have become less variable and there is an overall trend towards more negative $\delta^{34}S$.

The concentration of iron was the analyte most clearly affected by sediment loading. Comparing iron concentrations (Figure 10) with those amounts normalized for mass accumulation (Figure 11) it becomes clear how much of an effect dilution can have on the data. In Figure 10 both Fe_T and Fe_{HR} appear to almost completely disappear, as if all of the iron was somehow removed from the system after settlement, when in fact when corrected for sediment loading (Figure 11) it becomes clear there is actually more Fe in the system post-settlement than before. The increase in sediment in-washing into Martin Lake masked the authigenic enrichment of Fe after settlement. This means that although there was more Fe being incorporated post-settlement, detrital dilution during enhanced sedimentation rates artificially lowered the absolute concentrations. Average Fe_T (F) throughout the core was 1.3%, and Fe_{HR} (F) was 0.6%. The averages for Fe_T and Fe_{HR} were both higher after 1840 (1.8% and 0.6%, respectively) than before (0.9% and 0.3% respectively).

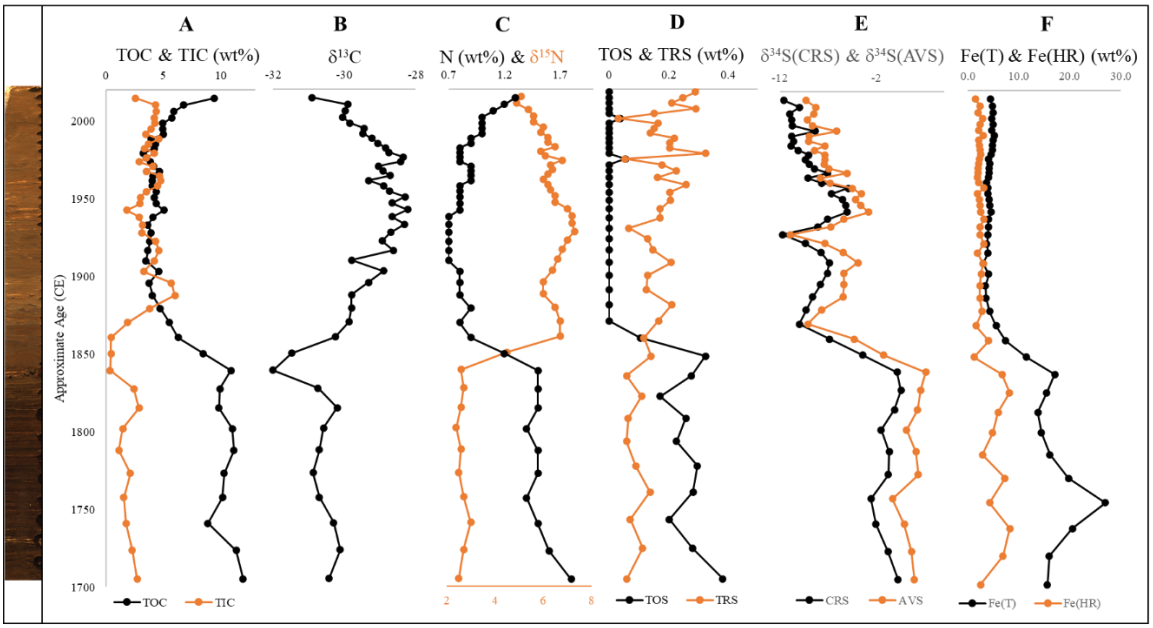

Figure 10: Summary of data collected from Martin Lake. **A**) wt% TOC (black) and TIC (orange), **B**) $\delta^{13}C$, **C**) wt% N (black) and $\delta^{15}N$ (orange), **D**) wt% TOS (black) and TRS (orange), **E**) $\delta^{34}S_{(CRS)}$ (black) and $\delta^{34}S_{(AVS)}$ (orange), **F**) wt% Fe_T (black) and Fe_{HR} (orange) plotted against the approximant age (CE). An image of the core accompanies the graphs on the left-hand side of the figure.

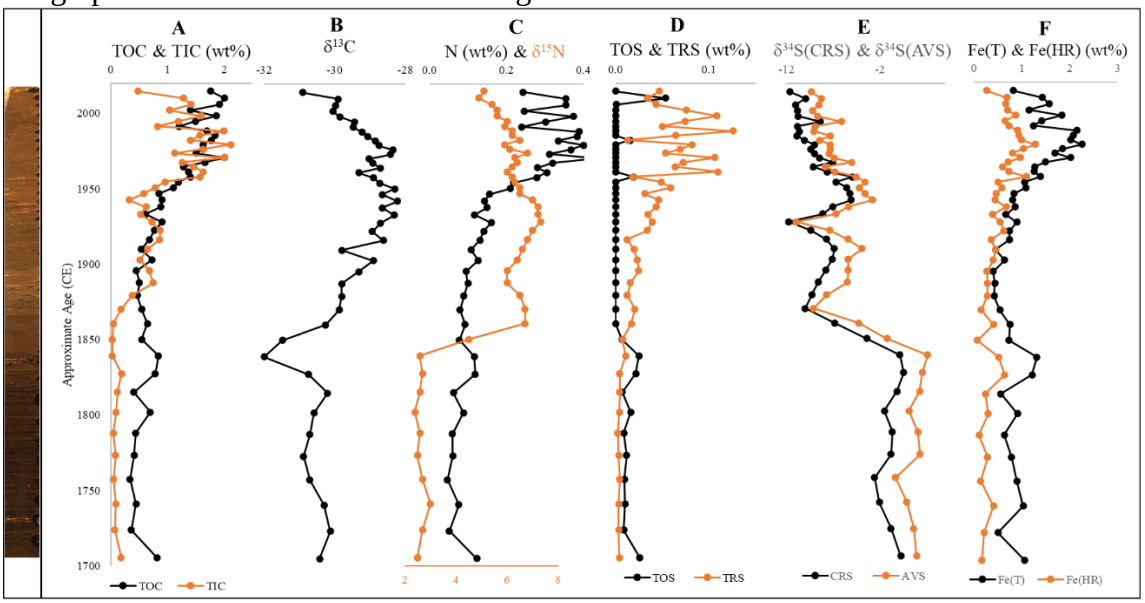

Figure 11: Summary of data collected from Martin Lake, standardized to mass accumulation rate. **A**) wt% TOC (black) and TIC (orange), **B**) $\delta^{13}C$, **C**) wt% N and $\delta^{15}N$ (orange), **D**) wt% TOS (black) and TRS (orange), **E**) $\delta^{34}S_{(CRS)}$ (black) and $\delta^{34}S_{(AVS)}$ (orange), **F**) Fe_T (black) and Fe_{HR} (orange) plotted against the approximant age (CE). All values measured in wt% have been standardized via the mass accumulation rate, isotope data remains the same as in Figure 10. An image of the core accompanies the graphs on the left-hand side of the figure.

2.5.5 Organic Nitrogen

In order to determine whether the total concentration of nitrogen in samples was derived from organic matter or inorganic nitrogen sources, such as ammonia bound into clays, the N (wt%) was plotted against TOC (wt%) in Figure 12. If there is a positive relationship that intercepts the origin, then the amount of nitrogen is proportional to the amount of TOC and therefore likely bound in organic matter (Schubert and Calvert, 2001). Conversely, a regression trend that passes through the y-axis would indicate that nitrogen is in excess of the organic matter available in the sediments. There is a strong positive correlation between TOC and N (R^2 = 0.9378) and the regression has an intercept of essentially zero (-0.0281% N) at 0% TOC. This relationship indicates that N in the samples is bound in organic matter with minimal contributions from clays or siliciclastic material. The bulk $\delta^{15}N$ values therefore represent the isotopic composition of organic nitrogen stored in the sediments, which is a direct record of organic matter input to the sediments.

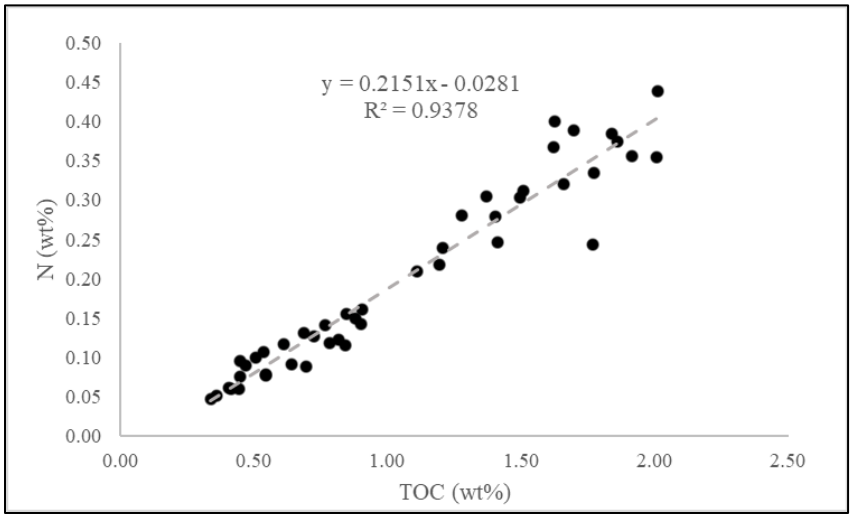

Figure 12: N (wt%) vs TOC (wt%). Y-intercept value is close to zero (-0.0281), and the R^2 value is 0.9378.

2.6 Discussion

The purpose of this research was to address an important question in limnology and forest management: what effect does deforestation have on the redox conditions of a lake? Deforestation is an important cross-discipline issue that has been well researched; however, the consequences of forest management practices remain to be fully studied

within the context of evolving redox conditions and lake ecology. Redox conditions are important to water quality and lake habitat (McMahon and Chapelle, 2008), which is why the lack of research in how deforestation affects this needs to be amended in order to have a more holistic view of the effects of deforestation. Paleoredox conditions in lakes are an important part of understanding the history of a lake regarding the interactions between the hydrosphere, biosphere, and geosphere. The previous studies of the Martin Lake water column and sediments (Wetzel, 1966; Bird et al., 2017), provides an ideal data archive with which to apply and calibrate the use of the iron redox proxies in this lake. Lessons learned from this study could then be applied to other lakes with similar histories of land clearance.

2.6.1 Increased Erosion After Land Clearance

Forest canopies effectively absorb the kinetic energy of impacting raindrops which protects the soil from the initiation of erosion caused by splash (Brant, 1988). Removing the tree cover during deforestation exposes soils to direct impact from falling precipitation. Sediment movement is markedly increased until some low plants or grasses are able to grow and dampen erosional effects to some extent. Soil sediment movement occurs as a direct result of the impacting raindrops, the sealing and crusting of the soil surface initiating overland flow and by increasing the turbulence of over-land flow (Brant, 1988). Greater precipitation or amplified erosion increase the movement of detritus (e.g. magnetic-rich minerals) from the lake's surrounding drainage basin into the lake environment (Brant, 1988; Kirby et al., 2004). Therefore, magnetic susceptibility typically increases as values correlate with either more precipitation washing sediment in or the land has been altered (deforested) and has become more easily eroded, also causing more sediment to wash into the lake. This is seen in the magnetic susceptibility conducted during this study of Martin Lake (Figure 8A). Around the time of colonial settlement in 1840 there is a clear increase in the magnetic susceptibility that continues to increase and remains much more variable than the baseline values from the pre-settlement era. This interpretation of increased runoff triggered by land clearance is also supported by the lithics data collected from the Bird et. al (2017), where post settlement

% lithics is well above the pre-settlement baseline (Figure 9C). The large increase in both magnetic susceptibility and lithics is a clear indication of the deforestation, and subsequently the increase in erosion of the Martin Lake watershed.

Beginning in 1840, there was an increase in mass accumulation (Figure 9A), consistent with the increase in magnetic susceptibility and lithics data that happened after colonial settlement. The increase in post-settlement sedimentation is the reason for normalizing geochemical data (Figure 10) to the accumulation rate (Figure 11). In Figure 10 post settlement values are much lower than in Figure 11 in which the values have been standardized to account for the increased sediment loading that is diluting the true representation of the values. This dilution only effects values that are in terms of weight percent, thus isotopic values remain unchanged between standardized and unstandardized figures. By correcting the concentration data for changes in sedimentation rate, we henceforth can use this data as a more accurate indication of environmental change.

2.6.2 Perturbation of the Carbon Cycle

The removal of forested cover by natural and man-made environmental disturbances can leave the landscape barren of the vegetation that once was prolific. Bulk $\delta^{13}C_{org}$ values of sedimentary organic matter deposited in lakes has been shown to be a reliable proxy to reconstruct important environmental changes in the distribution of terrestrial vegetation due to changes in climatic conditions (e.g., Talbot et al., 1992; Giresse et al.,1994; Ficken et al., 2002). Organic carbon isotopes have also been used to track anthropogenic environmental changes that would have caused a change in dominant plant species, such as deforestation or agriculture (e.g., Lane et al., 2004; Kerr et al., 2019; Wu et al., 2019). Secondary succession is the process in which an ecosystem develops on barren surfaces that have been cleared of most vegetation but still has its preexisting soil (Walker and Del Moral, 2003). Changes in vegetation within a deforested area occur quickly in the first years after deforestation and slowly progress from there to a new ecological state (Papp, 1987). Often, secondary vegetation is very different from the primary; improved drainage, clear cutting, selective cutting, grazing

and fires may totally change the character of the forest vegetation (Gordon, 1936; Reiners et al., 1994; Garcia-Vega and Newbold, 2020).

Directly following deforestation, the herb layer (herbaceous plants: grasses, ferns, wildflowers, and other low stature groundcover) dominates the landscape (Papp, 1987). Over time, more woody intermediate species such as shrubs and small trees will emerge through the perennials and grasses. Typically logging, either selective or clear cut, results in little arboreal re-growth and a prevalence of herbaceous species (Jenkins et al., 2013). Over decades the forest can reach its equilibrium point where species composition resembles pre-deforestation, although Martin Lake's watershed has yet to return to a fully forested state. A pattern of partial secondary succession can be seen clearly in the $\delta^{13}C_{org}$ data (Figure 11B). Pre-1840 $\delta^{13}C_{org}$ averaged -30.7‰, which is well within the range of woody C_3 plants (Meyers, 1994). After the deforestation, in 1840, there is a clear trend of increasing $\delta^{13}C_{org}$ values, which peaked in the late 1930's then decreased to pre-deforestation values. There is a clear 2‰ positive shift in $\delta^{13}C_{org}$ post settlement up until the late 1970s, which is clearly visible above baseline, pre-1840 levels. An increase towards higher $\delta^{13}C_{org}$ values shows an increased proportion of C_4 plants contributing to the organic carbon pool. Beginning around the late 1970s $\delta^{13}C_{org}$ values began to slowly decrease as more woody shrubs and trees reemerged. The use of clear-cut land for agriculture is likely; farming would also contribute to increased $\delta^{13}C_{org}$ values. Just as Native Americans had relied on corn for subsistence American settlers also grew corn as a main crop. The 1840 census revealed Kentucky, Tennessee, and Virginia to be the leading corn states, but within two decades that concentration had shifted northwestward and Indiana was top five in corn production (Edwards, 1941). Corn is a C4 plant; a heavy reliance on corn would be evident in the carbon isotope record as an increase in $\delta^{13}C_{org}$ values, such as what is seen during the post settlement, secondary succession period. The catchment today is still used for agriculture; however, the tributaries and the southern shorelines are completely forested (Figure 1A). The transition to lower $\delta^{13}C_{org}$ likely represents an increasing contribution of secondary regrowth.

Pollen data from a previous study by Williams (1974) of neighboring Pretty Lake also shows the same effect of colonial settlement land use history in the LaGrange region. Pretty Lake is part of a chain of kettle lakes and is approximately 14.5 km to the northeast

of Martin Lake. Today, Pretty Lake is associated with an oak-hickory region, since the patches of uncleared woodland near the lake are composed primarily of oaks, hickory, sugar maple, poplar, sycamore, dogwood, hackberry, sassafras, boxelder, and elm (Williams, 1974). This association is very similar to the pre-settlement vegetation of northeastern Indiana in about 1820, as described in a study based upon the original General Land Office Survey records and modern soil maps of Indiana counties, which correlated major soil types with forest subtypes (Lindsey et al., 1965). The time period 1280-1800 CE, was described as the "Quercus and Carya Maximum," where there was an increase in Quercus (oak) and Carya (hickory) pollen and a decrease in other arboreal pollen; this is the same type of forest that was recorded by early surveyors in the area in around the 1800s (Lindsey et al., 1965).

1800 CE to Present day was described by Williams (1974) as a period of "Dramatic Ambrosia Rise." This time period is characterized by a general increase in non-arboreal pollen particularly weed-types such as Ambrosia (ragweed; $\delta^{13}C$ = -18.7‰; Smedley et al., 1991), Plantago ($\delta^{13}C$ = -28.0‰; Fitter et al., 1998), and Rumex (dock weed; $\delta^{13}C$ = -29.8‰; Jumpponen et al., 2005). The Plantago species is believed to be one of the first plants introduced in North America after colonization and was commonly known by the Native Americans as the "white-man's footprint," because it thrived in the disturbed and damaged ecosystems surrounding colonial settlements (Duke, 2001). This onset of "weedy" vegetation reflects the effect that forest clearance and colonial agricultural practices had on the area. Thus, this zone represents the arrival of colonial settlers into the Pretty Lake region and subsequently, the Martin Lake region. Other pollen studies that cover the Late Holocene vegetation record in the general Midwest region (King and Allen, 1977; King, 1981) show similar patterns in gross vegetation, although exact plant species may vary locally.

2.6.3 Alteration of Nutrient Inputs

Martin Lake shows clear evidence of anthropogenic nitrogen loading from several plausible sources after colonial settlement. Anthropogenic effects can profoundly influence the nitrogen cycle; the burning of fossil fuels, agriculture, and urban development have increasingly released atmospheric and dissolved nitrogen into the environment (Vitousek et al., 1997). Anthropogenic nitrogen is highly mobile and can overprint the natural variability of atmospheric N_2, thus historical records of human induced $\delta^{15}N$ changes stand out well above background nitrogen levels (Last and Smol, 2002). A variety of lake records, spanning 100-200 years, have shown a clear trend of increasing $\delta^{15}N$ that correlates with population growth (Last and Smol, 2002). Population growth in Indiana within the region of Martin Lake, spurred by colonial settlement (Sieber and Munson, 1992), brought an increase in agriculture runoff and human waste, both of which have relatively high $\delta^{15}N$ values, into the lake. Organic fertilizer $\delta^{15}N$ ranges from 0.6 to 36.7‰, with farmyard manures having the highest mean $\delta^{15}N$ value (8.1‰) and largest range 3.5 to 16.2‰ (Bateman and Kelly, 2007). In comparison, synthetic fertilizers, derived from atmospheric nitrogen, that are commonly used today fall within a narrow range between −2 and +2‰ (Bateman and Kelly, 2007). Nitrogen derived from sewage has very high $\delta^{15}N$ values of 5 to 20‰ (Owens, 1988; Cabana and Rasmussen, 1996). Deforestation and agriculture also release soil N, which would also cause an increase in $\delta^{15}N$ as exemplified by a 3‰ increase reported for the effects of logging within the watershed of Walden Pond in Massachusetts (Köster et al.; 2005).

As seen in the data from Martin Lake (Figure 11D), $\delta^{15}N$ increased significantly after deforestation. Prior to colonial settlement, the average $\delta^{15}N$ value was 2.6‰, which falls within the range of organic fertilizer or natural soil nitrate, which usually ranges from 2 to 8‰ (McClelland & Valiela, 1998). Post settlement and deforestation, $\delta^{15}N$ values rose to an average of 6.2‰, likely from a combination of different sources of nitrate. Human and animal waste, which would have been an increasing concern as the population of LaGrange grew post-colonial settlement, have high $\delta^{15}N$ values. A

comparison of $\delta^{15}N$ values at these levels to the modern peak suggests that the watershed population could have been as large as 100 people/km^2 (Cabana and Rarmussen, 1996). This, in combination with an increase in released soil N due to deforestation (Nodvin et al., 1988), indicates a profound alteration of the nutrient cycle within the catchment of Martin Lake after development of the region by colonial settlers (Figure 13C). The slight decrease in $\delta^{15}N$ values back to pre-settlement values is consistent with the more modern practice of synthetic fertilizer application, which tends to have $\delta^{15}N$ values near 0‰, relative to organics (Bateman and Kelly, 2007).

2.6.4 Total Organic Carbon and C/N

Traditionally, weight percent N has been used for the understanding of lake nutrients (Guildford and Hecky, 2000), and the ratio of C/N has been used to distinguish sources of organic matter (Meyers, 1994). TOC in lake sediments is a bulk value that represents the fraction of organic matter that escaped remineralization during sedimentation (Meyers and Horie, 1993). TOC is widely used as a proxy to describe lake productivity in addition to use for studying changes in lacustrine palaeoproductivity, preservation, and depositional processes (Schelske and Hodeli, 1991; Ficken et al., 2002). Sharp changes in TOC concentrations are most often related to a change in preservation, amount of organic matter, or a change in algal productivity (Das et al., 2008). Anoxia decreases bacterial decomposition of organic matter throughout the water column, thus increasing the amount of preserved organic carbon within the sediment. An increase in TOC is likely caused after deforestation as erosion and runoff increased. C/N ratios can be used to distinguish the origin of OM, whether from algae or C_3 land plants, as they have much different ratios of 0-10 and 25-75, respectively (Meyers, 1994). This can be used in conjunction with TOC as a proxy for algal productivity. High TOC values with a low C/N ratio would be representative of high algal productivity (Ficken et al., 2002; Das et al., 2008).

Figure 13 shows a clear divide in the pre and post settlement nutrient composition of Martin Lake. The pre-settlement values cluster together, with little variability, and overall trend towards lower C/N values (Figure 13). Post settlement there is much wider

variability throughout the data, but an overall increase in C/N, $\delta^{15}N$, and $\delta^{13}C$. There has been a steady increase in TOC, especially in the past 100 years (Figure 11A), which provides a linear relationship with C/N (Figure 13A; $R^2 = 0.863$), showing that an increase in carbon is producing an increase in C/N values between pre and post settlement. Higher C/N values throughout the post settlement era coincide with an increase in $\delta^{13}C$ values (Figure 13B). This supports that deforestation caused an increased source of carbon (i.e. plant matter) and that the subsequent $\delta^{13}C$ values from the secondary regrowth throughout the watershed post settlement was heavily influenced by C4 plants, causing an overall increase in $\delta^{13}C$ values. Although there has been a clear increase in C/N values, overall C/N remains relatively low throughout.

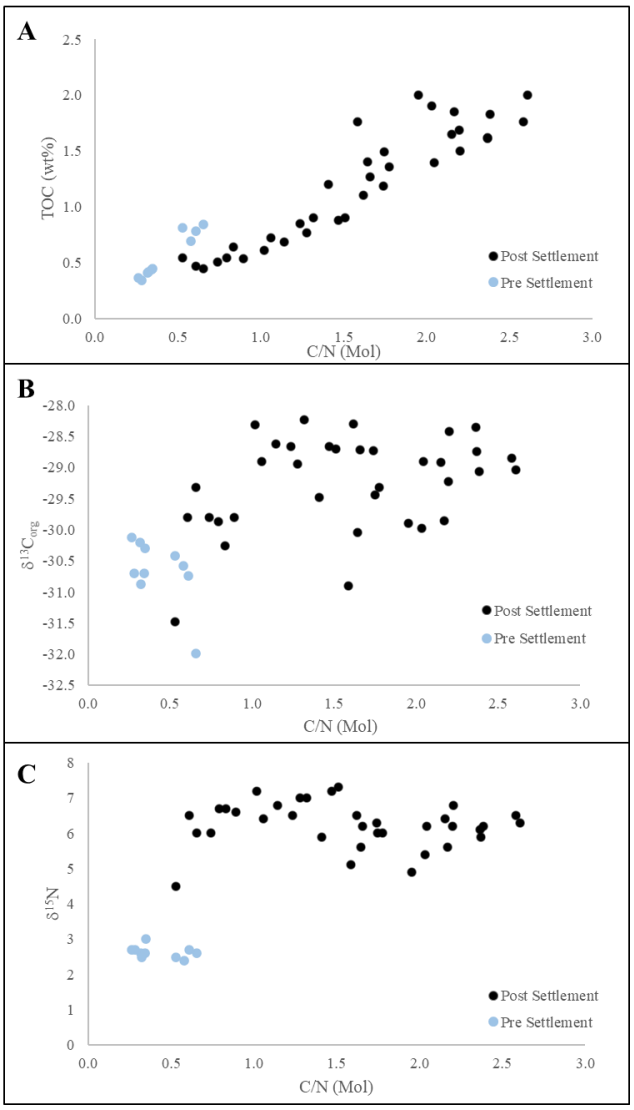

Figure 13: Relationships between elemental and isotopic compositions of organic carbon and nitrogen in Martin Lake. **A**) TOC (wt%) vs C/N (Mol). **B**) $\delta^{13}C_{org}$ vs C/N (Mol). **C**) $\delta^{15}N$ vs C/N (Mol). In all three panels, post settlement values are plotted in black and all pre settlement values are in blue.

2.6.5 Records of Water Column Redox

2.6.5.1 The Modern Water Column

These combined effects of increased erosion and input of organic matter and nitrogen into Martin Lake that coincide with colonial settlement of the region likely drove changes in water column redox not readily ascertained by traditional geochemical techniques.

More nutrients stimulates productivity within the lake, higher sedimentation rates lead to more rapid burial, more organic matter leads to greater decomposition and oxygen consumption. Combined, these three factors lead to oxygen deficiency. Today, the chemical condition of the water column is ferruginous. Martin Lake is seasonally anoxic at depth, has no detectable free dissolved sulfide, and has free dissolved Fe within the anoxic zone of the lake (Figure 6). Martin Lake water column sulfate concentrations are 0.2-0.3 mM with a $\delta^{34}S_{sulfate}$ value of -2.9‰ (Gilhooly, unpublished). Other metals data from Figure 6 show an increase in both P and Mn below the oxic zone. Dissolved Mn increased as oxygen was consumed, then P and Fe concentrations increased at the depth where oxygen was fully consumed. When there is very low oxygen, Mn oxides will dissolve and release dissolved Mn into the water, as oxygen is consumed to even lower levels Fe oxides will then dissolve. The P is typically bound to the Fe-oxides so it too will go into solution when Fe oxides dissolve (Slomp et al., 1996).

2.6.5.2 An Increase in Sulfate Availability After Settlement

Although the modern water column of Martin Lake is ferruginous, the surficial sediments exhibit fine laminations of light and dark sediments, and these sediments contain iron sulfides. Under these iron-rich conditions, the extent that dissolved iron can be reacted to form pyrite is dependent upon sulfate availability. The sulfide produced during microbial decay of organic matter and the dissolved iron released during reductive dissolution are the precursors to pyrite. The concentrations and sources of these two components can vary wildly over many different aquatic environments, accordingly the environmental factors resulting in these variations are an important piece to the understanding of lake redox history. The amount of pyrite that can form is limited by that amount of decomposable organic matter, dissolved sulfate, and reactive iron. In freshwater sediments, pyrite formation is typically limited by low concentrations of sulfate (Berner, 1984). Sulfide is created from the microbial reduction of sulfate; this indirect relationship between sulfate and pyrite is important in a lake system that is limited in one of the two components of pyrite. As seen in Figure 15, it is clear that pyrite is a minor fraction (less than 3%) of the reactive iron pool, indicating that sulfate is

the limiting factor for pyrite formation in Martin Lake. Meaning that there is an abundance of available Fe_{HR} relative to sulfate, under which conditions any free dissolved sulfide will likely immediately react with Fe_{HR} to create pyrite. The modern water column (Figure 6B) shows that there is free dissolved Fe in the water column. Over time the amount of pyrite has slightly increased (Figure 11E) meaning that there has been a slight increase in the amount of Fe-S species.

Sulfur isotope ($\delta^{34}S$) of iron sulfides in the sediment, may be a reflection of sulfate reduction in the water column or the sediment and the availability of sulfate (Farrell et al., 2013; Gilhooly et al, 2016). A change in the total amount of sulfate available can influence large positive and negative shifts in $\delta^{34}S$ that can be used to track the sulfate reservoir size and redox conditions of the water column (Gill et al., 2007). Bacteriogenic pyrite displays a wide range of values because sulfate reducing bacteria preferentially break ^{32}S-bonds during microbial sulfate reduction resulting in sulfide with low $\delta^{34}S$. Sulfate reducing bacteria are strictly anaerobic and occur in anoxic sediments, producing sulfide (Ibanez et al., 2010). In anoxic sediments, hydrogen sulfide with low $\delta^{34}S$ values, inherited from microbial sulfate reduction combines with Fe_{HR} to form pyrite above or below the sediment-water interface. Pyrite formation has minimal fractionation (Price and Shieh, 1979) and therefore the isotope composition of iron sulfides in the sediments is a faithful record of the precursor sulfide. Fractionation is dependent on sulfate concentration and the sulfate reduction rate. At lower concentrations, somewhere between 50 µM and around 200 µM, the sulfate reduction rate is suppressed, decreasing fractionation (Habicht et al., 2002). Martin Lake has a sulfate concentration of 200-300 µM, suggesting that the extent of fractionation between sulfate and the sulfide produced during microbial reduction is generally small, but not negligible.

Within Martin Lake, the sulfur retained in the sediment switches from primarily organic sulfur to almost entirely iron sulfides (TRS) after deforestation (Figure 11E). The average concentration of organic sulfur (0.02%) prior to colonial settlement dropped substantially to 0.003% after deforestation. The average pre-settlement isotope composition of AVS ($\delta^{34}S$ = 1.8‰) and CRS ($\delta^{34}S$ = -0.8‰) was higher than those in the overlying sediments (Fig 11F). After deforestation, both $\delta^{34}S_{AVS}$ and $\delta^{34}S_{CRS}$ decreased to -6.5‰ and -8.5‰, respectively (Figure 11F). A possible explanation for pronounced

transition to lower $\delta^{34}S$ in both AVS and CRS is that the concentration of sulfate increased after 1840.

The increase in sulfate availability inferred from the progressive decrease in $\delta^{34}S$ values of mineral sulfides is potentially linked to land use change. Long-term, deforestation and regrowth may lower the acidity of the soil through strong nitrate retention which decreases the ability of the soil to retain sulfate (Nodvin et al., 1988). On the centennial scale, this can cause stream water sulfate to reach a new equilibrium of higher concentrations than prior to deforestation (Forti et al., 1994), showing that the effects of deforestation can reside long after the forests have regrown. As the concentration of AVS and pyrite increased in post-settlement sediment, the isotope composition of these sulfide phases decreased (Figure 14 A and B). Pre-settlement values cluster towards low levels of pyrite and AVS with small, near zero, $\delta^{34}S$. Post settlement values exhibit greater variability, likely from variability in the sulfate reservoir, but overall exhibit an increase in both concentration and $\delta^{34}S_{AVS}$ and $\delta^{34}S_{CRS}$. In addition to an increase in sulfate availability, higher concentrations of labile organic matter, from the increased erosion post deforestation (which is supported by the TOC values) were buried in the more recent sediments. This means that a larger portion of organic matter is available for sulfate reduction, resulting in an increased $\delta^{34}S_{CRS}$ fractionation (Figure 14C; Pasquier et al., 2017). An increase in TOC in combination with an increase in the fractionation of $\delta^{34}S_{CRS}$ shows that the increase in sulfate availability is most likely from a lack of soil retention post deforestation.

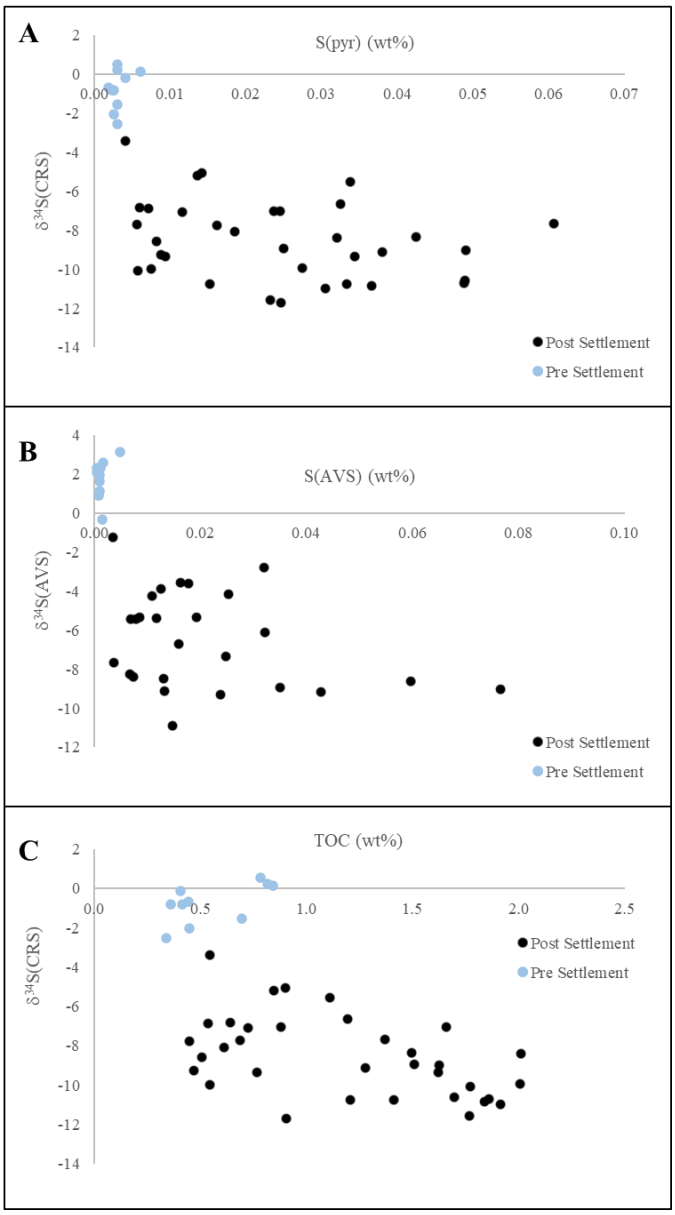

Figure 14: Relationships between elemental and isotopic compositions of sedimentary sulfides in Martin Lake. **A**) $\delta^{34}S_{pyr}$ versus S_{pyr} (wt%). **B**) $\delta^{34}S_{AVS}$ versus S_{AVS} (wt%). **C**) $\delta^{34}S_{pyr}$ versus TOC (wt%). In all panels, pre-settlement values are in blue and post settlement values are in black.

2.6.5.3 Reactive Iron

Iron redox proxies have long been an essential tool in marine studies, here we have modified them to show that they can also be an essential part of the lacustrine toolkit. Because Martin Lake's geochemistry is much different in concentration than the marine

systems that the iron redox proxies were developed from, the relative change in these ratios in the lake sediment record are more informative than the empirical ratios. Rather than use the marine threshold value of 0.38 as the determinant for the presence or absence of oxygen (Raiswell and Canfield, 1998), oxic conditions in Martin Lake are marked by low levels of Fe_{HR} compared to Fe_T, whereas a relative enhancement of Fe_{HR} would be expected under anoxic conditions. An anoxic system that has a relatively minor fraction of Fe_{HR} converted to pyrite is indicative of a ferruginous environment in which the reactive Fe supply was greater than the titrating capacity of hydrogen sulfide, meaning that no excess hydrogen sulfide accumulates in the water column (Reinhard et al., 2013). Figure 16 shows the relative change in baseline ratios pre-settlement and post settlement. Fe_{HR}/Fe_T values pre-settlement average 0.017 ± 0.012 and increase significantly to 0.143 (Figure 16A). This order of magnitude increase in the ratio shows that the amount of Fe_{HR} has increased relative to Fe_T after settlement; asserting that conditions in Martin Lake became more reducing after settlement and deforestation of the watershed. Figure 15 shows that the relative abundance of Fe_{HR} species ($Fe_{HR} = Fe_{carb} + Fe_{ox} + Fe_{mag} + Fe_{pyr} + Fe_{AVS}$) increased after settlement. An intensification in sedimentation after deforestation likely increased the deposition of Fe into the lake. Since the 1980's, there has been a trend of decreasing Fe_{HR} relative to Fe_T (Figure 16), trending towards baseline levels. Sedimentation rate had rapidly declined since the 1980s (Figure 9B), probably in part to the Olin Lake becoming a nature preserve in the mid-1970s. Martin Lake connects to Olin Lake via an outlet to the west. The nature preserve protects 341 acres of land, including the southern shoreline of Martin Lake. A decrease in erosion likely changed the chemistry of the water flowing into the lake. $^{34}S_{AVS}$ and $\delta^{34}S_{CRS}$ values continued to decrease in the most recent sediments, indicating that the lake chemistry of Martin Lake transitioned to a new "normal."

Based on these modified iron redox proxies Martin Lake experienced increased seasonal stratification, due to the end of the LIA, and more robust anoxic/ferruginous conditions due to a change in water chemistry after settlement and deforestation. The Fe_{pyr}/Fe_{HR} baseline before settlement, averaged near zero (0.001 ± 0.0003), which means despite the availability of at least some reactive iron in the system a negligible fraction of it was being converted into pyrite. The proportions of pyrite increased ten-fold after

settlement (Figure 16B). Figure 11A shows that at the same time pyrite increased that Fe_{HR} increased as well, meaning that not only was there more reactive iron available, but more of it was able to react to form pyrite. As mentioned before an increase in sulfate availability after deforestation is likely the cause for the increase in pyrite. The increase in Fe_{HR} in combination with the modern water column samples showing free dissolved Fe in the water column (Figure 6B) show that Martin Lake overtime has become a ferruginous lake, due to the changes in the post settlement watershed. A cross-plot of Fe_{HR}/Fe_T and Fe_{pyr}/Fe_{HR} (Figure 17) clearly shows the difference in pre and post settlement conditions. Pre-settlement values show little variability and cluster towards low reactive Fe availability and basically no pyrite. Post settlement values show a much wider range, but generally show an increase in both available Fe and an increase in pyrite.

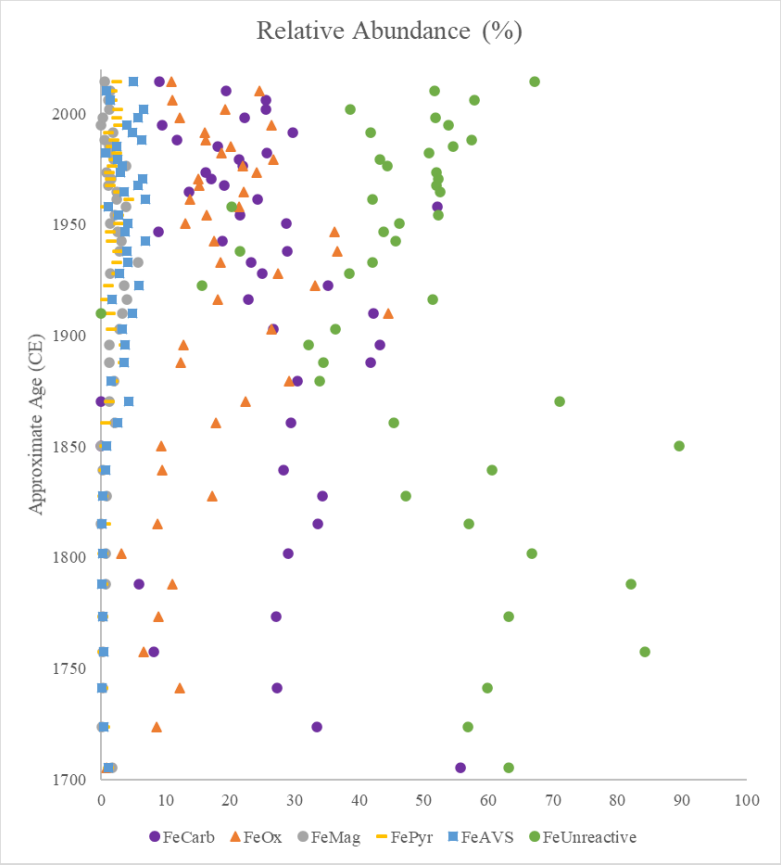

Figure 15: Relative abundance of each iron species throughout the core. Carbonates (purple), oxides (orange), magnetite (grey), pyrite (yellow), AVS (light blue), and the unreactive portion (green).

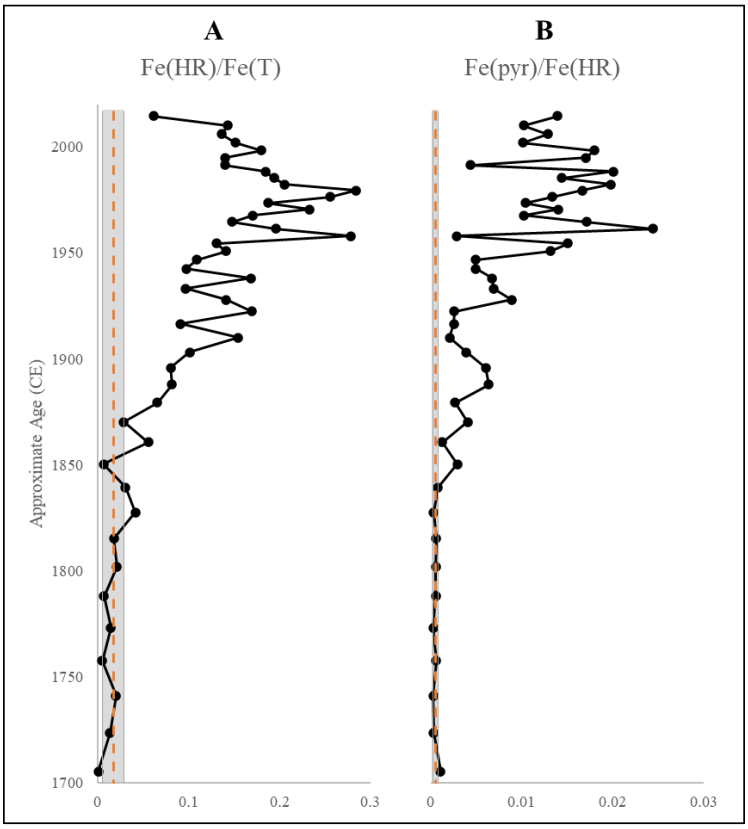

Figure 16: Martin Lake Fe_{HR}/Fe_T and Fe_{pyr}/Fe_{HR} ratios. (**A**) The ratio of highly reactive iron to total iron (Fe_{HR}/Fe_T) and (**B**) the ratio of pyrite to highly reactive iron (Fe_{pyr}/Fe_{HR}) throughout the age of the core. Values for both graphs have been standardized using the mass accumulation rate. Dashed orange line represents the average value pre-1840 for each ratio; grey bars represent ± one standard deviation.

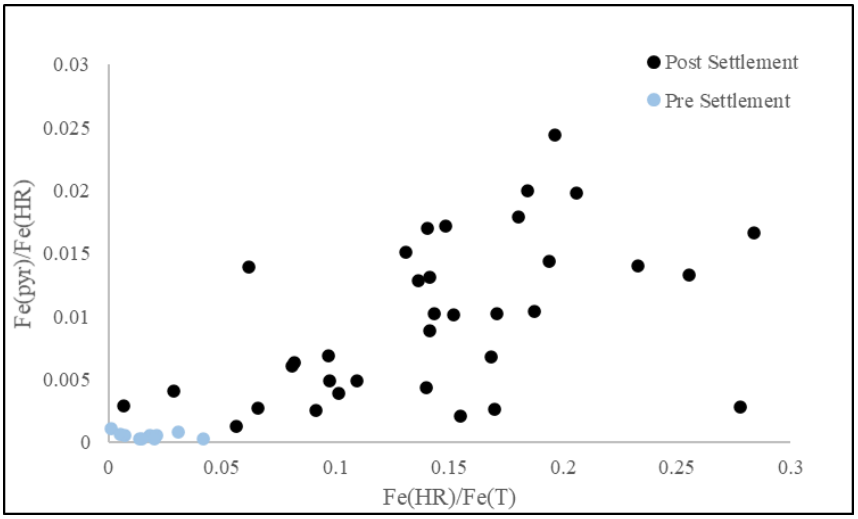

Figure 17: The ratio of pyrite to highly reactive iron (Fe_{pyr}/Fe_{HR}) vs the ratio of highly reactive iron to total iron (Fe_{HR}/Fe_T). Post settlement values are plotted in black and pre settlement values are in blue.

2.7 Summary and Conclusions

Human activity has greatly modified biogeochemical cycles and global environmental change. These effects include the alteration of the natural landscape, the creation of synthetic fertilizers, the increasing extinction rate of plant and animal species, and the continued consumption of fossil fuels (Crutzen, 2006; Barnosky et al., 2011; Dirzo et al., 2014). It has been argued that due to the breadth and permanency of these human-induced changes in the Holocene Epoch that the Earth has now moved into what has been called the Anthropocene (Crutzen and Stoermer, 2000; Crutzen, 2002; Steffen and Crutzen, 2007). The chemostratigraphic record of Martin Lake reveal the effects of colonial settlement within a small catchment. These localized impacts when considered on the global scale, reveal profound changes to aquatic biogeochemical cycles since the Industrial Revolution. My research shows a clear shift in the geochemical characteristics of Martin Lake before and after settlement, as revealed through the changes in isotope values and redox conditions, that can be directly attributed to anthropogenic causes.

This study revealed that even a small (relative to today), pre-industrial population can rapidly and permanently alter the redox state of a lacustrine environment. The post settlement conditions of Martin Lake show a stark contrast to the forested watershed that surrounded the area before 1840. The impacts of settlement can be seen through the lenses of all of the proxies that were used in this study. **1**) Deforestation post settlement increased the erosion of the surrounding land, increasing the sedimentation rate and the % lithics. **2**) $\delta^{13}C$ of organic matter reveals a pattern of deforestation and partial regrowth and agricultural use of land. **3**) An increase in population at the time of settlement can be seen through the rise in $\delta^{15}N$ values from the increase of waste into Martin Lake. **4**) TOC and C/N show an overall increase in organic carbon matter into the lake caused by deforestation, and that the increased nutrient supply may have stimulated more in-lake productivity. **5**) $\delta^{34}S$ values show that deforestation lead to an increase in the available sulfate pool of Martin Lake, which in combination with **6**) an increase in Fe_{HR} created an environment in which pyrite formation was more favorable. These observations make it evident that there was a shift in the biogeochemistry of Martin Lake driven by anthropogenic alterations to the watershed post settlement. At this time though, the

record remains unclear whether these factors ultimately changed water column redox to the anoxic/ferruginous conditions observed today. The shifts in Fe_{HR} and pyrite after settlement suggest changes in redox biogeochemistry; however, it is difficult to determine the extent of oxygen deficiency that may have occurred throughout the Martin Lake record presented here. Additional context such as independent constraints on lake water pH and residence time, as well as high resolution sedimentological descriptions that can characterize laminations and the presence/absence of bioturbation, are needed to calibrate iron speciation data as a record of lake water paleo-redox.

2.8 Chapter 2 References

Abel, D. C., Koenig, C. C., & Davis, W. P. (1987). Emersion in the mangrove forest fishRivulus marmoratus: a unique response to hydrogen sulfide. Environmental Biology of Fishes, 18(1), 67-72.

Adrian, R., O'Reilly, C. M., Zagarese, H., Baines, S. B., Hessen, D. O., Keller, W., ... & Weyhenmeyer, G. A. (2009). Lakes as sentinels of climate change. Limnology and oceanography, 54(6part2), 2283-2297.

Anderson, R. Y. (1985). Meromictic lakes and varved lake sediments in North America (No. 1607). US Government Printing Office.

Andrew J, T., Norman D, Y., Keller, B., Girard, R., Heneberry, J., Gunn, J. M., ... & Taylor, P. A. (2008). Cooling lakes while the world warms: Effects of forest regrowth and increased dissolved organic matter on the thermal regime of a temperate, urban lake. Limnology and Oceanography, 53(1), 404-410.

Andrews, J. E., Riding, R., & Dennis, P. F. (1993). Stable isotopic compositions of recent freshwater cyanobacterial carbonates from the British Isles: local and regional environmental controls. Sedimentology, 40(2), 303-314.

Andrews, J. E., Riding, R., & Dennis, P. F. (1997). The stable isotope record of environmental and climatic signals in modern terrestrial microbial carbonates from Europe. Palaeogeography, Palaeoclimatology, Palaeoecology, 129(1-2), 171-189.

Angelsen, A., & Kaimowitz, D. (1999). Rethinking the causes of deforestation: lessons from economic models. The world bank research observer, 14(1), 73-98.

Barbier, E. B., & Burgess, J. C. (2001). The economics of tropical deforestation and land use: an introduction to the special issue. Land Economics, 77(2), 155-171.

Barnosky, A. D., Matzke, N., Tomiya, S., Wogan, G. O., Swartz, B., Quental, T. B., ... & Mersey, B. (2011). Has the Earth's sixth mass extinction already arrived?. Nature, 471(7336), 51-57.

Bateman, A. S., & Kelly, S. D. (2007). Fertilizer nitrogen isotope signatures. Isotopes in environmental and health studies, 43(3), 237-247.

Berner, R. A. (1984). Sedimentary pyrite formation: an update. Geochimica et cosmochimica Acta, 48(4), 605-615.

Bird, B. W., Wilson, J. J., Gilhooly III, W. P., Steinman, B. A., & Stamps, L. (2017). Midcontinental Native American population dynamics and late Holocene hydroclimate extremes. Scientific Reports, 7, 41628.

Bonan, G. B. (2008). Forests and climate change: forcings, feedbacks, and the climate benefits of forests. science, 320(5882), 1444-1449.

Brandt, J. (1988). The transformation of rainfall energy by a tropical rain forest canopy in relation to soil erosion. Journal of Biogeography, 41-48.

Brodie, C. R., Leng, M. J., Casford, J. S., Kendrick, C. P., Lloyd, J. M., Yongqiang, Z., & Bird, M. I. (2011). Evidence for bias in C and N concentrations and δ13C composition of terrestrial and aquatic organic materials due to pre-analysis acid preparation methods. Chemical Geology, 282(3-4), 67-83.

Burton, G. A., Green, A., Baudo, R., Forbes, V., Nguyen, L. T., Janssen, C. R., ... & Kapo, K. (2007). Characterizing sediment acid volatile sulfide concentrations in European streams. Environmental toxicology and chemistry, 26(1), 1-12.

Cabana, G., & Rasmussen, J. B. (1996). Comparison of aquatic food chains using nitrogen isotopes. Proceedings of the National Academy of Sciences, 93(20), 10844-10847.

Canfield, D. E., Raiswell, R., Westrich, J. T., Reaves, C. M., & Berner, R. A. (1986). The use of chromium reduction in the analysis of reduced inorganic sulfur in sediments and shales. Chemical geology, 54(1-2), 149-155.

Cook, R. B., & Kelly, C. A. (1989). Sulfur cycling and fluxes in temperate dimictic lakes (No. CONF-8905327-1). Oak Ridge National Lab., TN (USA).

Cox, E.T. (Ed.) (1874). Fifth Annual Report of the Geological Survey of Indiana. Indianapolis, IN: Sentinel Company, Printers.

Crutzen, P. J. (2002). Geology of mankind. Nature 415.

Crutzen, P. J. (2006). The “anthropocene”. In Earth system science in the anthropocene (pp. 13-18). Springer, Berlin, Heidelberg.

Crutzen, P. J., & Stoermer, E. F. (2000). The Anthropocene, Global change newsletter. 41, 17-18. *International Geosphere–Biosphere Programme (IGBP)*.

Das, S. K., Routh, J., Roychoudhury, A. N., & Klump, J. V. (2008). Elemental (C, N, H and P) and stable isotope (δ 15 N and δ 13 C) signatures in sediments from Zeekoevlei, South Africa: a record of human intervention in the lake. Journal of Paleolimnology, 39(3), 349-360.

Dirzo, R., Young, H. S., Galetti, M., Ceballos, G., Isaac, N. J., & Collen, B. (2014). Defaunation in the Anthropocene. science, 345(6195), 401-406.

Duke, J. A. (2001). CRC Handbook of edible weeds.

Edwards, E. E. (1941). American agriculture: the first 300 years. US Department of Agriculture.

Farrell, Ú. C., Briggs, D. E., Hammarlund, E. U., Sperling, E. A., & Gaines, R. R. (2013). Paleoredox and pyritization of soft-bodied fossils in the Ordovician Frankfort Shale of New York. American Journal of Science, 313(5), 452-489.

Ficken, K. J., Wooller, M. J., Swain, D. L., Street-Perrott, F. A., & Eglinton, G. (2002). Reconstruction of a subalpine grass-dominated ecosystem, Lake Rutundu, Mount Kenya: a novel multi-proxy approach. Palaeogeography, Palaeoclimatology, Palaeoecology, 177(1-2), 137-149.

Ficker, H., Luger, M., & Gassner, H. (2017). From dimictic to monomictic: empirical evidence of thermal regime transitions in three deep alpine lakes in Austria induced by climate change. Freshwater Biology, 62(8), 1335-1345.

Fitter, A. H., Graves, J. D., Watkins, N. K., Robinson, D., & Scrimgeour, C. (1998). Carbon transfer between plants and its control in networks of arbuscular mycorrhizas. Functional Ecology, 12(3), 406-412.

Forti, M. C., Neal, C., & Jenkins, A. (1995). Modeling perspective of the deforestation impact in stream water quality of small preserved forested areas in the Amazonian rainforest. Water, Air, and Soil Pollution, 79(1-4), 325-337.

France, R. (1997). Land water linkages: influences of riparian deforestation on lake thermocline depth and possible consequences for cold stenotherms. Canadian Journal of Fisheries and Aquatic Sciences, 54(6), 1299-1305.

García-Vega, D., & Newbold, T. (2020). Assessing the effects of land use on biodiversity in the world's drylands and Mediterranean environments. Biodiversity and Conservation, 29(2), 393-408.

Gilhooly III, W. P., Reinhard, C. T., & Lyons, T. W. (2016). A comprehensive sulfur and oxygen isotope study of sulfur cycling in a shallow, hyper-euxinic meromictic lake. Geochimica et Cosmochimica Acta, 189, 1-23.

Gill, B. C., Lyons, T. W., & Saltzman, M. R. (2007). Parallel, high-resolution carbon and sulfur isotope records of the evolving Paleozoic marine sulfur reservoir. Palaeogeography, Palaeoclimatology, Palaeoecology, 256(3-4), 156-173.

Giresse, P., Maley, J., & Brenac, P. (1994). Late Quaternary palaeoenvironments in the Lake Barombi Mbo (West Cameroon) deduced from pollen and carbon isotopes of organic matter. Palaeogeography, Palaeoclimatology, Palaeoecology, 107(1-2), 65-78.

Golosov, S., Terzhevik, A., Zverev, I., Kirillin, G., & Engelhardt, C. (2012). Climate change impact on thermal and oxygen regime of shallow lakes. Tellus A: Dynamic Meteorology and Oceanography, 64(1), 17264.

Gordon, R. (1936). A Preliminary Vegetation Map of Indiana. The American Midland Naturalist, 17(5), 866-877. doi:10.2307/2420692

Guildford, S. J., & Hecky, R. E. (2000). Total nitrogen, total phosphorus, and nutrient limitation in lakes and oceans: Is there a common relationship?. Limnology and Oceanography, 45(6), 1213-1223.

Habicht, K. S., Gade, M., Thamdrup, B., Berg, P., & Canfield, D. E. (2002). Calibration of sulfate levels in the Archean ocean. Science, 298(5602), 2372-2374.

Hughen, K. A., Overpeck, J. T., & Anderson, R. F. (2000). Recent warming in a 500-year palaeotemperature record from varved sediments, Upper Soper Lake, Baffin Island, Canada. The Holocene, 10(1), 9-19.

Ibanez, J. G., Hernandez-Esparza, M., Doria-Serrano, C., Fregoso-Infante, A., & Singh, M. M. (2010). Environmental chemistry: fundamentals. Springer Science & Business Media.

Jenkins, M. A. (2013). The history of human disturbance in forest ecosystems of southern Indiana. In: Swihart, Robert K.; Saunders, Michael R.; Kalb, Rebecca A.; Haulton, G. Scott; Michler, Charles H., eds. 2013. The Hardwood Ecosystem Experiment: a framework for studying responses to forest management. Gen.

Tech. Rep. NRS-P-108. Newtown Square, PA: US Department of Agriculture, Forest Service, Northern Research Station: 2-11., 2-11.

Jumpponen, A., Mulder, C. P. H., Huss-Danell, K., & Högberg, P. (2005). Winners and losers in herbaceous plant communities: insights from foliar carbon isotope composition in monocultures and mixtures. Journal of Ecology, 93(6), 1136-1147.

Kerr, M. T., Horn, S. P., & Lane, C. S. (2019). Stable isotope analysis of vegetation history and land use change at Laguna Santa Elena in southern Pacific Costa Rica. Vegetation History and Archaeobotany, 1-16.

King, J. E. (1981). Late Quaternary vegetational history of Illinois. Ecological Monographs, 51(1), 43-62.

King, J. E., & Allen, W. H. (1977). A Holocene vegetation record from the Mississippi River Valley, southeastern Missouri. Quaternary Research, 8(3), 307-323.

Kirby, M. E., Poulsen, C. J., Lund, S. P., Patterson, W. P., Reidy, L., & Hammond, D. E. (2004). Late Holocene lake level dynamics inferred from magnetic susceptibility and stable oxygen isotope data: Lake Elsinore, southern California (USA). Journal of Paleolimnology, 31(3), 275-293.

Koeksoy, E., Halama, M., Konhauser, K. O., & Kappler, A. (2016). Using modern ferruginous habitats to interpret Precambrian banded iron formation deposition. International Journal of Astrobiology, 15(3), 205-217.

Konhauser, K. O., Gingras, M. K., & Kappler, A. (2011). Sediment Diagenesis–Biologically Controlled. In Encyclopedia of Geobiology.

Köster, D., Pienitz, R., Wolfe, B. B., Barry, S., Foster, D. R., & Dixit, S. S. (2005). Paleolimnological assessment of human-induced impacts on Walden Pond (Massachusetts, USA) using diatoms and stable isotopes. Aquatic Ecosystem Health & Management, 8(2), 117-131.

Lane, C. S., Horn, S. P., & Mora, C. I. (2004). Stable carbon isotope ratios in lake and swamp sediments as a proxy for prehistoric forest clearance and crop cultivation in the Neotropics. Journal of Paleolimnology, 32(4), 375-381.

Last, W. M., & Smol, J. P. (Eds.). (2002). Tracking Environmental Change Using Lake Sediments: Volume 2: Physical and Geochemical Methods (Vol. 2). Springer Science & Business Media.

Leathers, D. J., Yarnal, B., & Palecki, M. A. (1991). The Pacific/North American teleconnection pattern and United States climate. Part I: Regional temperature and precipitation associations. Journal of Climate, 4(5), 517-528.

Leng, M. J., & Marshall, J. D. (2004). Palaeoclimate interpretation of stable isotope data from lake sediment archives. Quaternary Science Reviews, 23(7-8), 811-831.

Leonard, E. N., Mattson, V. R., Benoit, D. A., Hoke, R. A., & Ankley, G. T. (1993). Seasonal variation of acid volatile sulfide concentration in sediment cores from three northeastern Minnesota lakes. Hydrobiologia, 271(2), 87-95.

Lindsey, A. A., Crankshaw, W. B., & Qadir, S. A. (1965). Soil relations and distribution map of the vegetation of presettlement Indiana. *Botanical Gazette*, *126*(3), 155-163.

Lorion, C. M., & Kennedy, B. P. (2009). Relationships between deforestation, riparian forest buffers and benthic macroinvertebrates in neotropical headwater streams. Freshwater biology, 54(1), 165-180.

Lyons, T. W., & Severmann, S. (2006). A critical look at iron paleoredox proxies: New insights from modern euxinic marine basins. Geochimica et Cosmochimica Acta, 70(23), 5698-5722.

Lyons, T. W., Werne, J. P., Hollander, D. J., & Murray, R. W. (2003). Contrasting sulfur geochemistry and Fe/Al and Mo/Al ratios across the last oxic-to-anoxic transition in the Cariaco Basin, Venezuela. Chemical Geology, 195(1), 131-157.

McClelland, J. W., & Valiela, I. (1998). Linking nitrogen in estuarine producers to land-derived sources. Limnology and Oceanography, 43(4), 577-585.

McMahon, P. B., & Chapelle, F. H. (2008). Redox processes and water quality of selected principal aquifer systems. Groundwater, 46(2), 259-271.

Meyers, P. A. (1994). Preservation of elemental and isotopic source identification of sedimentary organic matter. Chemical geology, 114(3-4), 289-302.

Meyers, P. A., & Horie, S. (1993). An organic carbon isotopic record of glacial-postglacial change in atmospheric pCO2 in the sediments of Lake Biwa, Japan. Palaeogeography, Palaeoclimatology, Palaeoecology, 105(3-4), 171-178.

Meyers, P. A., & Lallier-Vergès, E. (1999). Lacustrine sedimentary organic matter records of Late Quaternary paleoclimates. Journal of Paleolimnology, 21(3), 345-372.

Myers, N. (2002). Environmental refugees: a growing phenomenon of the 21st century. Philosophical Transactions of the Royal Society of London B: Biological Sciences, 357(1420), 609-613.

Nebbioso, A., & Piccolo, A. (2013). Molecular characterization of dissolved organic matter (DOM): a critical review. Analytical and bioanalytical chemistry, 405(1), 109-124.

New, J. F. Oliver, Olin, and Martin Lakes diagnostic study La Grange County, Indiana. 280 (2009).

Nodvin, S. C., Driscoll, C. T., & Likens, G. E. (1988). Soil processes and sulfate loss at the Hubbard Brook Experimental Forest. Biogeochemistry, 5(2), 185-199.

Oseid, D. M., & Smith JR, L. L. (1974). Chronic toxicity of hydrogen sulfide to Gammarus pseudolimnaeus. Transactions of the American Fisheries Society, 103(4), 819-822.

Owens, J. D., Lyons, T. W., Li, X., Macleod, K. G., Gordon, G., Kuypers, M. M., ... & Severmann, S. (2012). Iron isotope and trace metal records of iron cycling in the proto-North Atlantic during the Cenomanian-Turonian oceanic anoxic event (OAE-2). Paleoceanography and Paleoclimatology, 27(3).

Owens, N. J. P. (1988). Natural variations in 15N in the marine environment. In Advances in marine biology (Vol. 24, pp. 389-451). Academic Press.

Papp, M. (1987). A six year study of a secondary succession after deforestation in North Hungary. Folia Geobotanica et Phytotaxonomica, 22(4), 405-413.

Pasquier, V., Sansjofre, P., Rabineau, M., Revillon, S., Houghton, J., & Fike, D. A. (2017). Pyrite sulfur isotopes reveal glacial− interglacial environmental changes. Proceedings of the National Academy of Sciences, 114(23), 5941-5945.

Poulton, S. W., & Canfield, D. E. (2005). Development of a sequential extraction procedure for iron: implications for iron partitioning in continentally derived particulates. Chemical Geology, 214(3-4), 209-221.

Poulton, S. W., & Canfield, D. E. (2011). Ferruginous conditions: a dominant feature of the ocean through Earth's history. Elements, 7(2), 107-112.

Price, F. T., & Shieh, Y. N. (1979). Fractionation of sulfur isotopes during laboratory synthesis of pyrite at low temperatures. Chemical Geology, 27(3), 245-253.

Raiswell, R., & Canfield, D. E. (1998). Sources of iron for pyrite formation in marine sediments. American Journal of Science, 298(3), 219-245.

Raiswell, R., Buckley, F., Berner, R. A., & Anderson, T. F. (1988). Degree of pyritization of iron as a paleoenvironmental indicator of bottom-water oxygenation. Journal of Sedimentary Research, 58(5), 812-819.

Raiswell, R., Hardisty, D. S., Lyons, T. W., Canfield, D. E., Owens, J. D., Planavsky, N. J., ... & Reinhard, C. T. (2018). The iron paleoredox proxies: A guide to the pitfalls, problems and proper practice. American Journal of Science, 318(5), 491-526.

Rask, M., Arvola, L., & Salonen, K. (1993). Effects of catchment deforestation and burning on the limnology of a small forest lake in southern Finland. Internationale Vereinigung für theoretische und angewandte Limnologie: Verhandlungen, 25(1), 525-528.

Read, J. S., & Rose, K. C. (2013). Physical responses of small temperate lakes to variation in dissolved organic carbon concentrations. Limnology and Oceanography, 58(3), 921-931.

Reiners, W. A., Bouwman, A. F., Parsons, W. F. J., & Keller, M. (1994). Tropical rain forest conversion to pasture: changes in vegetation and soil properties. Ecological Applications, 4(2), 363-377.

Reinhard, C. T., Lyons, T. W., Rouxel, O., Asael, D., Dauphas, N., & Kump, L. R. (2013). Iron speciation and isotope perspectives on palaeoproterozoic water column chemistry. In Reading the Archive of Earth's Oxygenation - Volume 3: Global Events and the Fennoscandian Arctic Russia -Drilling Early Earth Project (pp. 1483-1492). (Frontiers in Earth Sciences; Vol. 8). Frontiers. DOI: 10.1007/978-3-642-29670-3_10

Rico, K. I., & Sheldon, N. D. (2019). Nutrient and iron cycling in a modern analogue for the redoxcline of a Proterozoic ocean shelf. Chemical Geology.

Rogers, J. C., & Coleman, J. S. (2003). Interactions between the Atlantic Multidecadal Oscillation, El Nino/La Nina, and the PNA in winter Mississippi valley stream flow. Geophysical Research Letters, 30(10).

Romanek, C. S., Grossman, E. L., & Morse, J. W. (1992). Carbon isotopic fractionation in synthetic aragonite and calcite: effects of temperature and precipitation rate. Geochimica et cosmochimica acta, 56(1), 419-430.

Rosenmeier, M. F., Hodell, D. A., Brenner, M., Curtis, J. H., & Guilderson, T. P. (2002). A 4000-year lacustrine record of environmental change in the southern Maya lowlands, Peten, Guatemala. Quaternary Research, 57(2), 183-190.

Schelske, C. L., & Hodeli, D. A. (1991). Recent changes in productivity and climate of Lake Ontario detected by isotopic analysis of sediments. Limnology and Oceanography, 36(5), 961-975.

Schubert, C. J., & Calvert, S. E. (2001). Nitrogen and carbon isotopic composition of marine and terrestrial organic matter in Arctic Ocean sediments:: implications for nutrient utilization and organic matter composition. Deep Sea Research Part I: Oceanographic Research Papers, 48(3), 789-810.

Sieber, E., & Munson, C. A. (1992). Looking at history: Indiana's Hoosier National Forest region, 1600 to 1950. US Dept. of Agriculture, Forest Service.

Slomp, C. P., Van der Gaast, S. J., & Van Raaphorst, W. (1996). Phosphorus binding by poorly crystalline iron oxides in North Sea sediments. Marine Chemistry, 52(1), 55-73.

Smedley, M. P., Dawson, T. E., Comstock, J. P., Donovan, L. A., Sherrill, D. E., Cook, C. S., & Ehleringer, J. R. (1991). Seasonal carbon isotope discrimination in a grassland community. Oecologia, 85(3), 314-320.

Solomon, C. T., Jones, S. E., Weidel, B. C., Buffam, I., Fork, M. L., Karlsson, J., ... & Saros, J. E. (2015). Ecosystem consequences of changing inputs of terrestrial dissolved organic matter to lakes: current knowledge and future challenges. Ecosystems, 18(3), 376-389.

Steedman, R. J., France, R. L., Kushneriuk, R. S., & Peters, R. H. (1998). Effects of riparian deforestation on littoral water temperatures in small boreal forest lakes. Boreal Environment Research, 3, 161-170.

Steffen, W., Crutzen, P. J., & McNeill, J. R. (2007). The Anthropocene: are humans now overwhelming the great forces of nature. *AMBIO: A Journal of the Human Environment*, *36*(8), 614-622.

Talbot, M. R., & Johannessen, T. (1992). A high resolution palaeoclimatic record for the last 27,500 years in tropical West Africa from the carbon and nitrogen isotopic composition of lacustrine organic matter. Earth and Planetary Science Letters, 110(1-4), 23-37.

Tomkins, J. D., Antoniades, D., Lamoureux, S. F., & Vincent, W. F. (2008). A simple and effective method for preserving the sediment–water interface of sediment cores during transport. Journal of Paleolimnology, 40(1), 577-582.

Vitousek, P. M., Aber, J. D., Howarth, R. W., Likens, G. E., Matson, P. A., Schindler, D. W., ... & Tilman, D. G. (1997). Human alteration of the global nitrogen cycle: sources and consequences. Ecological applications, 7(3), 737-750.

Walker, L. R., & Del Moral, R. (2003). Primary succession and ecosystem rehabilitation. Cambridge University Press.

Wetzel, R. G. (1966). Productivity and nutrient relationships in marl lakes of northern Indiana: With 2 figures and 6 tables in the text. Internationale Vereinigung für theoretische und angewandte Limnologie: Verhandlungen, 16(1), 321-332.

Wetzel, R.G. (1973) Productivity investigations of interconnected lakes. I. The eight lakes of the Oliver and Walters chains, northeastern Indiana. Hydrobiology Studies, 3, 91-143.

Williams, A. S. (1974). Late-glacial-postglacial vegetational history of the Pretty Lake region, northeastern Indiana (No. 686-B). US Govt. Print. Off.,.

Williamson, C. E., Dodds, W., Kratz, T. K., & Palmer, M. A. (2008). Lakes and streams as sentinels of environmental change in terrestrial and atmospheric processes. Frontiers in Ecology and the Environment, 6(5), 247-254.

Wu, J., Porinchu, D. F., & Horn, S. P. (2019). Late Holocene hydroclimate variability in Costa Rica: Signature of the terminal classic drought and the Medieval Climate Anomaly in the northern tropical Americas. Quaternary Science Reviews, 215, 144-159.

Wuebbles, D. J., & Hayhoe, K. (2004). Climate change projections for the United States Midwest. Mitigation and Adaptation Strategies for Global Change, 9(4), 335-363.

APPENDIX

Depth (m)	Temp (C)	pH	Dissolved O (mg/L)	Salinity (ppt)	Turbidity (NTU)	Mn (ppb)	P (ppb)	Fe (ppb)
0	21.00	9.21	9.63	0.28	4.9			
1	20.50	9.23	9.81	0.28	4.9	79.1	135.86	63.8
2	17.83	9.02	9.91	0.29	5.7			
3	9.24	9.32	14.43	0.29	6.4	52.0	126.76	58.1
4	9.85	9.31	13.72	0.29	7.4			
5	6.87	9.22	12.34	0.29	8.1	46.8	127.46	51.22
6	6.46	9.41	11.00	0.29	8.8			
7	6.23	9.09	10.19	0.29	9.3	59.0	123.45	49.42
8	6.00	9.05	9.85	0.29	9.5			
9	5.63	9.02	9.55	0.29	9.6	105.1	121.78	48.37
10	5.35	8.99	9.00	0.29	9.2	46.2	122.60	55.14
11	4.85	8.88	7.51	0.30	9.7	51.9	122.35	47.66
12	4.50	8.23	4.15	0.31	9.7	354.2	122.43	51.11
13	4.15	8.62	0	0.32	9.8	1412.8	124.61	49.60
14	4.03	8.59	0	0.33	10.7	2926.9	130.72	56.04
15	4.01	8.53	0	0.34	14.2	5366.1	1026.93	29885.23
16	4.01	8.57	0	0.34	33.0	4432.7	907.24	20665.81

Table A: Martin Lake water column data.

Sample	Depth (cm)	Empty Boat (g)	Wet Total (g)	Dry Total (g)	Bulk Density (g/cm3)	Year (CE)	Sedimentation Rate (cm/yr)	Mass Accumulation Rate (g/cm2/yr)
1	1	0.646	1.333	0.816	0.517	2014.6	0.36	0.19
2	3	0.654	1.681	0.914	0.767	2010.2	0.39	0.30
3	5	0.661	1.720	0.950	0.770	2006.0	0.42	0.32
4	7	0.608	1.359	0.817	0.542	2002.0	0.45	0.25
5	9	0.739	1.811	1.051	0.760	1998.3	0.49	0.37
6	11	0.671	1.482	0.909	0.573	1994.8	0.53	0.30
7	13	0.698	1.287	0.862	0.425	1991.5	0.56	0.24
8	15	0.698	1.731	1.007	0.724	1988.3	0.60	0.43
9	17	0.711	1.711	1.028	0.683	1985.3	0.62	0.43
10	19	0.701	1.663	1.015	0.648	1982.3	0.65	0.42
11	21	0.637	1.776	1.017	0.759	1979.3	0.66	0.50
12	23	0.763	1.812	1.119	0.693	1976.4	0.66	0.46
13	25	0.632	1.473	0.879	0.594	1973.5	0.66	0.39
14	27	0.653	1.708	0.948	0.760	1970.6	0.64	0.49
15	29	0.546	1.357	0.781	0.576	1967.6	0.62	0.36
16	31	0.566	1.343	0.812	0.531	1964.5	0.59	0.31
17	33	0.641	1.529	0.918	0.611	1961.3	0.55	0.34
18	35	0.647	1.654	0.981	0.673	1958.0	0.52	0.35
19	37	0.680	1.535	0.968	0.567	1954.5	0.48	0.27
20	39	0.720	1.606	1.016	0.590	1950.7	0.44	0.26
21	41	0.625	1.341	0.867	0.474	1946.8	0.41	0.19
22	43	0.671	1.381	0.907	0.474	1942.5	0.38	0.18
23	45	0.557	1.509	0.889	0.620	1938.0	0.35	0.21
24	47	0.656	1.481	0.955	0.526	1933.2	0.32	0.17
25	49	0.649	1.717	0.930	0.787	1928.0	0.29	0.23
26	51	0.649	1.772	1.021	0.751	1922.4	0.27	0.20
27	53	0.734	1.923	1.162	0.761	1916.4	0.25	0.19
28	55	0.725	1.768	1.091	0.677	1910.0	0.23	0.15
29	57	0.749	2.015	1.258	0.757	1903.1	0.21	0.16
30	59	0.694	1.553	0.939	0.614	1895.7	0.19	0.12
31	61	0.640	1.653	0.956	0.697	1887.8	0.18	0.12
32	63	0.658	1.575	0.977	0.598	1879.3	0.17	0.10
33	65	0.575	1.512	0.874	0.638	1870.2	0.15	0.10
34	67	0.618	1.677	0.965	0.712	1860.6	0.14	0.10
35	69	0.668	1.268	0.788	0.480	1850.2	0.13	0.06
36	71	0.632	1.391	0.773	0.618	1839.3	0.13	0.08
37	73	0.681	1.525	0.852	0.673	1827.6	0.12	0.08
38	75	0.801	1.274	0.897	0.377	1815.1	0.11	0.04
39	77	0.683	1.443	0.830	0.613	1802.0	0.10	0.06
40	79	0.645	1.151	0.742	0.409	1788.0	0.10	0.04
41	81	0.682	1.224	0.785	0.439	1773.2	0.09	0.04
42	83	0.677	1.151	0.764	0.387	1757.6	0.09	0.03
43	85	0.641	1.408	0.789	0.619	1741.1	0.08	0.05
44	87	0.615	1.133	0.719	0.414	1723.7	0.08	0.03
45	89	0.638	1.789	0.852	0.937	1705.3	0.07	0.07

Table B: Data for sedimentation rate and mass accumulation rate.

Sample	Depth (cm)	Year (CE)	FeCarb-FeAVS (wt%)	FeOx (wt%)	FeMag (wt%)	FePyr (wt%)	FeAVS (wt%)	Unreative Fe (wt%)	Fe(T) (wt%)	Fe(HR) (wt%)	Fe(HR)/ Fe(T)	Fe(pyr)/ Fe(HR)		Mass Accumulation Rate (g/cm2/yr)	FeCarb-FeAVS (wt%)	FeOx (wt%)	FeMag (wt%)	FePyr (wt%)	FeAVS (wt%)	Unreative Fe (wt%)	Fe(T) (wt%)	Fe(HR) (wt%)	Fe(HR) /Fe(T)	Fe(pyr)/ Fe(HR)
ML1	1	2014.6	0.40	0.48	0.02	0.11	0.22	2.97	4.42	1.45	0.33	0.07		0.19	0.07	0.09	0.00	0.02	0.04	0.56	0.83	0.27	0.06	0.01
ML2	3	2010.2	0.93	1.19	0.06	0.08	0.04	2.50	4.84	2.34	0.48	0.03		0.30	0.28	0.35	0.02	0.02	0.01	0.74	1.43	0.69	0.14	0.01
ML3	5	2006.0	1.25	0.54	0.05	0.08	0.07	2.83	4.89	2.06	0.42	0.04		0.32	0.40	0.17	0.02	0.03	0.02	0.91	1.58	0.67	0.14	0.01
ML4	7	2002.0	1.19	0.89	0.06	0.12	0.30	1.79	4.66	2.86	0.61	0.04		0.25	0.29	0.22	0.01	0.03	0.07	0.44	1.15	0.71	0.15	0.01
ML5	9	1998.3	1.09	0.59	0.01	0.11	0.28	2.54	4.90	2.36	0.48	0.05		0.37	0.41	0.22	0.00	0.04	0.10	0.95	1.83	0.88	0.18	0.02
ML6	11	1994.8	0.44	1.23	0.00	0.12	0.19	2.52	4.68	2.17	0.46	0.06		0.30	0.13	0.37	0.00	0.04	0.06	0.76	1.42	0.66	0.14	0.02
ML7	13	1991.5	1.55	0.84	0.09	0.06	0.26	2.17	5.21	3.04	0.58	0.02		0.24	0.37	0.20	0.02	0.01	0.06	0.52	1.25	0.73	0.14	0.00
ML8	15	1988.3	0.58	0.80	0.03	0.10	0.31	2.85	4.98	2.13	0.43	0.05		0.43	0.25	0.35	0.01	0.04	0.13	1.23	2.15	0.92	0.18	0.02
ML9	17	1985.3	0.87	0.97	0.06	0.07	0.11	2.65	4.86	2.21	0.45	0.03		0.43	0.37	0.41	0.03	0.03	0.05	1.13	2.07	0.94	0.19	0.01
ML10	19	1982.3	1.24	0.90	0.07	0.11	0.03	2.46	4.84	2.38	0.49	0.05		0.42	0.52	0.38	0.03	0.05	0.01	1.03	2.03	1.00	0.21	0.02
ML11	21	1979.3	0.96	1.20	0.09	0.09	0.12	1.95	4.51	2.56	0.57	0.03		0.50	0.48	0.60	0.04	0.04	0.06	0.97	2.25	1.00	0.28	0.02
ML12	23	1976.4	0.88	0.88	0.16	0.07	0.13	1.79	4.04	2.25	0.56	0.03		0.46	0.40	0.40	0.07	0.03	0.06	0.82	1.85	1.00	0.26	0.01
ML13	25	1973.5	0.70	1.04	0.04	0.06	0.13	2.26	4.34	2.09	0.48	0.03		0.39	0.27	0.41	0.01	0.02	0.05	0.88	1.69	0.81	0.19	0.01
ML14	27	1970.6	0.71	0.62	0.07	0.06	0.27	2.16	4.15	1.98	0.48	0.03		0.49	0.34	0.30	0.03	0.03	0.13	1.05	2.02	0.97	0.23	0.01
ML15	29	1967.6	0.80	0.63	0.04	0.06	0.24	2.18	4.20	2.02	0.48	0.03		0.36	0.28	0.23	0.02	0.02	0.09	0.77	1.49	0.72	0.17	0.01
ML16	31	1964.5	0.55	0.89	0.09	0.11	0.14	2.13	4.06	1.93	0.47	0.06		0.31	0.17	0.28	0.03	0.03	0.04	0.67	1.27	0.60	0.15	0.02
ML17	33	1961.3	0.90	0.51	0.09	0.16	0.25	1.56	3.72	2.16	0.58	0.07		0.34	0.30	0.17	0.03	0.05	0.09	0.53	1.26	0.73	0.20	0.02
ML18	35	1958.0	2.07	0.85	0.15	0.03	0.04	0.81	3.98	3.17	0.80	0.01		0.35	0.72	0.30	0.05	0.01	0.01	0.28	1.39	1.11	0.28	0.00
ML19	37	1954.5	0.84	0.64	0.08	0.10	0.10	2.04	3.91	1.87	0.48	0.06		0.27	0.23	0.17	0.02	0.03	0.03	0.56	1.07	0.51	0.13	0.02
ML20	39	1950.7	1.19	0.54	0.06	0.11	0.17	1.92	4.16	2.24	0.54	0.05		0.26	0.31	0.14	0.02	0.03	0.04	0.50	1.09	0.59	0.14	0.01
ML21	41	1946.8	0.38	1.54	0.11	0.06	0.16	1.87	4.29	2.41	0.56	0.03		0.19	0.07	0.30	0.02	0.01	0.03	0.36	0.83	0.47	0.11	0.00
ML22	43	1942.5	0.86	0.80	0.14	0.07	0.31	2.09	4.58	2.49	0.54	0.03		0.18	0.15	0.14	0.03	0.01	0.06	0.37	0.82	0.44	0.10	0.00
ML23	45	1938.0	1.16	1.47	0.11	0.10	0.16	0.86	4.02	3.15	0.78	0.03		0.21	0.25	0.31	0.02	0.02	0.03	0.19	0.86	0.68	0.17	0.01
ML24	47	1933.2	0.93	0.74	0.23	0.10	0.17	1.69	4.02	2.33	0.58	0.04		0.17	0.16	0.12	0.04	0.02	0.03	0.28	0.67	0.39	0.10	0.01
ML25	49	1928.0	0.98	1.07	0.05	0.09	0.11	1.50	3.92	2.42	0.62	0.04		0.23	0.22	0.25	0.01	0.02	0.03	0.34	0.90	0.55	0.14	0.01
ML26	51	1922.4	1.30	1.23	0.13	0.04	0.22	0.58	3.71	3.14	0.84	0.01		0.20	0.26	0.25	0.03	0.01	0.04	0.12	0.75	0.63	0.17	0.00
ML27	53	1916.4	0.90	0.72	0.16	0.03	0.06	2.04	3.98	1.93	0.49	0.01		0.19	0.17	0.13	0.03	0.00	0.01	0.38	0.75	0.36	0.09	0.00
ML28	55	1910.0	1.25	1.32	0.10	0.04	0.14	-0.02	2.97	3.00	1.01	0.01		0.15	0.19	0.20	0.02	0.01	0.02	0.00	0.46	0.46	0.15	0.00
ML29	57	1903.1	1.08	1.07	0.11	0.06	0.13	1.47	4.06	2.59	0.64	0.02		0.16	0.17	0.17	0.02	0.01	0.02	0.23	0.64	0.41	0.10	0.00
ML30	59	1895.7	1.48	0.44	0.04	0.12	0.13	1.10	3.43	2.33	0.68	0.05		0.12	0.18	0.05	0.00	0.01	0.01	0.13	0.41	0.28	0.08	0.01
ML31	61	1887.8	1.48	0.44	0.04	0.12	0.13	1.22	3.55	2.33	0.66	0.05		0.12	0.18	0.05	0.01	0.01	0.02	0.15	0.44	0.29	0.08	0.01
ML32	63	1879.3	1.30	1.24	0.08	0.08	0.06	1.45	4.28	2.83	0.66	0.03		0.10	0.13	0.12	0.01	0.01	0.01	0.14	0.42	0.28	0.07	0.00
ML33	65	1870.2	0.00	1.24	0.07	0.07	0.23	3.92	5.53	1.61	0.29	0.04		0.10	0.00	0.12	0.01	0.01	0.02	0.39	0.54	0.16	0.03	0.00
ML34	67	1860.6	2.18	1.31	0.15	0.05	0.19	3.36	7.42	4.06	0.55	0.01		0.10	0.22	0.13	0.02	0.01	0.02	0.34	0.76	0.42	0.06	0.00
ML35	69	1850.2	0.00	1.06	0.00	0.06	0.09	10.30	11.51	1.21	0.11	0.05		0.06	0.00	0.07	0.00	0.00	0.01	0.66	0.74	0.08	0.01	0.00
ML36	71	1839.3	4.81	1.60	0.03	0.07	0.11	10.30	17.03	6.73	0.40	0.01		0.08	0.37	0.12	0.00	0.01	0.01	0.80	1.32	0.52	0.03	0.00
ML37	73	1827.6	5.30	2.66	0.12	0.03	0.04	7.30	15.48	8.19	0.53	0.00		0.08	0.42	0.21	0.01	0.00	0.00	0.57	1.22	0.64	0.04	0.00
ML38	75	1815.1	4.60	1.19	0.00	0.09	0.02	7.81	13.73	5.92	0.43	0.01		0.04	0.19	0.05	0.00	0.00	0.00	0.32	0.57	0.24	0.02	0.00
ML39	77	1802.0	4.18	0.44	0.10	0.04	0.03	9.62	14.44	4.82	0.33	0.01		0.06	0.26	0.03	0.01	0.00	0.00	0.61	0.91	0.30	0.02	0.00
ML40	79	1788.0	0.94	1.76	0.10	0.04	0.02	13.20	16.08	2.88	0.18	0.01		0.04	0.04	0.07	0.00	0.00	0.00	0.52	0.64	0.11	0.01	0.00
ML41	81	1773.2	5.35	1.75	0.04	0.05	0.05	12.48	19.77	7.30	0.37	0.01		0.04	0.21	0.07	0.00	0.00	0.00	0.50	0.79	0.29	0.01	0.00
ML42	83	1757.6	2.19	1.78	0.06	0.08	0.08	22.72	27.00	4.27	0.16	0.02		0.03	0.07	0.06	0.00	0.00	0.00	0.76	0.90	0.14	0.01	0.00
ML43	85	1741.1	5.58	2.50	0.05	0.05	0.03	12.26	20.50	8.23	0.40	0.01		0.05	0.28	0.13	0.00	0.00	0.00	0.62	1.03	0.41	0.02	0.00
ML44	87	1723.7	5.32	1.36	0.02	0.07	0.05	9.06	15.94	6.88	0.43	0.01		0.03	0.17	0.04	0.00	0.00	0.00	0.29	0.51	0.22	0.01	0.00
ML45	89	1705.3	0.99	1.38	0.02	0.04	0.03	15.61	2.48	0.16	0.02	0.02		0.00	0.00	0.00	0.00	0.00	0.00	0.00	0.00	0.00	0.00	0.00

Table C: Iron species data and reactive iron proxy data in both unstandardized and standardized form.

Sample	Depth (cm)	Year (CE)	TC (wt%)	TIC (wt%)	TOC (wt%)	TOS (wt%)	TS (wt%)	S-pyr (wt%)	S-AVS (wt%)	TRS (wt%)	δ13C	δ34S(CRS)	δ34S(AVS)	δ15N	N (wt%)	C/N (Mol)	Fe(T) (wt%)	Fe(HR) (wt%)		Mass Accumulation Rate (g/cm2/yr)	TC (wt%)	TIC (wt%)	TOC (wt%)	TOS (wt%)	TS (wt%)	S-pyr (wt%)	S-AVS (wt%)	TRS (wt%)	N (wt%)	C/N (Mol)	Fe(T) (wt%)	Fe(HR) (wt%)
ML1	1	2014.6	12.03	2.59	9.44	0	0.002	0.12	0.13	0.25	-30.9	-11.6	-9.3	5.1	1.3	8.5	4.4	1.5		0.19	2.25	0.49	1.77	0.00	0.00	0.02	0.02	0.05	0.24	1.58	0.83	0.27
ML2	3	2010.2	11.14	4.35	6.79	0.18	0.30	0.09	0.02	0.12	-29.9	-9.9	-8.2	4.9	1.2	6.6	4.8	2.3		0.30	3.30	1.29	2.01	0.05	0.09	0.03	0.01	0.03	0.36	1.95	1.43	0.69
ML3	5	2006.0	10.31	4.37	5.93	0.002	0.14	0.09	0.04	0.13	-30.0	-11.0	-8.5	5.4	1.1	6.3	4.9	2.1		0.32	3.33	1.41	1.92	0.00	0.04	0.03	0.01	0.04	0.36	2.03	1.58	0.67
ML4	7	2002.0	9.93	4.21	5.72	0	0.16	0.13	0.17	0.31	-30.0	-10.8	-9.2	5.6	1	6.7	4.7	2.9		0.25	2.45	1.04	1.41	0.00	0.04	0.03	0.04	0.08	0.25	1.64	1.15	0.71
ML5	9	1998.3	9.24	4.27	4.98	0	0.12	0.13	0.16	0.29	-29.9	-10.7	-8.6	5.6	1	5.8	4.9	2.4		0.37	3.45	1.59	1.86	0.00	0.04	0.05	0.06	0.11	0.37	2.17	1.83	0.88
ML6	11	1994.8	8.90	3.95	4.95	0	0.08	0.14	0.11	0.25	-29.4	-8.3	-6.1	6.0	1	5.8	4.7	2.2		0.30	2.69	1.20	1.50	0.00	0.03	0.04	0.03	0.07	0.30	1.75	1.42	0.66
ML7	13	1991.5	8.50	3.47	5.03	0	0.14	0.06	0.15	0.21	-29.5	-10.8	-8.9	5.9	1	5.9	5.2	3.0		0.24	2.04	0.83	1.21	0.00	0.03	0.02	0.04	0.05	0.24	1.41	1.25	0.73
ML8	15	1988.3	8.55	4.62	3.93	0	0.08	0.11	0.18	0.29	-29.2	-10.6	-9.0	6.2	0.9	5.1	5.0	2.1		0.43	3.69	2.00	1.70	0.00	0.04	0.05	0.08	0.13	0.39	2.20	2.15	0.92
ML9	17	1985.3	7.99	3.68	4.31	0	0.07	0.09	0.07	0.15	-29.1	-10.8	-7.3	6.2	0.9	5.6	4.9	2.2		0.43	3.41	1.57	1.84	0.00	0.03	0.04	0.03	0.06	0.38	2.38	2.07	0.94
ML10	19	1982.3	7.60	3.37	4.24	0.04	0.07	0.01	0.02	0.03	-28.9	-10.1	-8.4	6.5	0.8	6.2	4.8	2.4		0.42	3.18	1.41	1.77	0.02	0.03	0.01	0.01	0.01	0.33	2.58	2.03	1.00
ML11	21	1979.3	7.49	4.23	3.25	0	0.07	0.10	0.07	0.16	-28.7	-9.0	-7.3	5.9	0.8	4.7	4.5	2.6		0.50	3.74	2.12	1.63	0.00	0.04	0.05	0.03	0.08	0.40	2.37	2.25	1.28
ML12	23	1976.4	7.09	3.56	3.54	0	0.07	0.08	0.08	0.15	-28.4	-9.3	-7.3	6.1	0.8	5.2	4.0	2.2		0.46	3.25	1.63	1.62	0.00	0.03	0.03	0.03	0.07	0.37	2.37	1.85	1.03
ML13	25	1973.5	6.76	2.88	3.88	0	0.07	0.06	0.07	0.14	-28.4	-8.9	-7.4	6.8	0.8	5.7	4.3	2.1		0.39	2.63	1.12	1.51	0.00	0.03	0.02	0.03	0.05	0.31	2.20	1.69	0.81
ML14	27	1970.6	8.26	4.12	4.13	0	0.13	0.07	0.15	0.22	-29.0	-8.4	-6.9	6.3	0.9	5.4	4.1	2.0		0.49	4.02	2.01	2.01	0.00	0.06	0.03	0.07	0.11	0.44	2.61	2.02	0.97
ML15	29	1967.6	8.22	3.55	4.67	0	0.12	0.07	0.14	0.20	-28.9	-7.0	-5.0	6.4	0.9	6.1	4.2	2.0		0.36	2.92	1.26	1.66	0.00	0.04	0.02	0.05	0.07	0.32	2.15	1.49	0.72
ML16	31	1964.5	8.79	4.69	4.10	0	0.11	0.12	0.08	0.20	-28.7	-9.1	-7.8	6.2	0.9	5.3	4.1	1.9		0.31	2.74	1.46	1.28	0.00	0.04	0.04	0.03	0.06	0.28	1.66	1.27	0.60
ML17	33	1961.3	8.84	4.80	4.04	0	0.10	0.18	0.14	0.32	-29.3	-7.7	-6.8	6.0	0.9	5.2	3.7	2.2		0.34	2.99	1.62	1.37	0.00	0.03	0.06	0.05	0.11	0.30	1.77	1.26	0.73
ML18	35	1958.0	8.54	4.52	4.02	0.05	0.11	0.03	0.02	0.05	-28.9	-4.9	-4.5	6.2	0.8	5.9	4.0	3.2		0.35	2.98	1.57	1.40	0.02	0.04	0.01	0.01	0.02	0.28	2.04	1.39	1.11
ML19	37	1954.5	7.89	3.51	4.38	0	0.09	0.12	0.06	0.18	-28.7	-6.7	-3.6	6.3	0.8	6.4	3.9	1.9		0.27	2.15	0.96	1.19	0.00	0.03	0.03	0.02	0.05	0.22	1.74	1.07	0.51
ML20	39	1950.7	7.23	3.00	4.23	0	0.07	0.13	0.10	0.23	-28.3	-5.5	-4.2	6.5	0.8	6.2	4.2	2.2		0.26	1.90	0.79	1.11	0.00	0.02	0.03	0.03	0.06	0.21	1.62	1.09	0.59
ML21	41	1946.8	7.33	2.97	4.36	0	0.09	0.07	0.09	0.16	-28.7	-5.2	-3.6	6.5	0.8	6.4	4.3	2.4		0.19	1.42	0.58	0.85	0.00	0.02	0.01	0.02	0.03	0.16	1.23	0.83	0.47
ML22	43	1942.5	6.86	1.81	5.06	0	0.10	0.08	0.18	0.26	-28.2	-5.1	-2.8	7.0	0.8	7.4	4.6	2.5		0.18	1.23	0.32	0.90	0.00	0.02	0.01	0.03	0.05	0.14	1.32	0.82	0.44
ML23	45	1938.0	7.02	2.91	4.11	0	0.07	0.11	0.09	0.20	-28.7	-7.0	-5.4	7.2	0.7	6.8	4.0	3.2		0.21	1.51	0.62	0.88	0.00	0.01	0.02	0.02	0.04	0.15	1.47	0.86	0.68
ML24	47	1933.2	6.84	3.17	3.67	0	0.05	0.11	0.10	0.21	-28.3	-8.1	-6.7	7.2	0.7	6.1	4.0	2.3		0.17	1.14	0.53	0.61	0.00	0.01	0.02	0.02	0.03	0.12	1.02	0.67	0.39
ML25	49	1928.0	7.10	3.15	3.95	0	0.07	0.11	0.06	0.17	-28.7	-11.7	-10.9	7.3	0.7	6.6	3.9	2.4		0.23	1.63	0.72	0.91	0.00	0.02	0.02	0.01	0.04	0.16	1.51	0.90	0.55
ML26	51	1922.4	8.16	4.34	3.82	0	0.08	0.05	0.12	0.17	-28.9	-9.4	-7.3	7.0	0.7	6.4	3.7	3.1		0.20	1.64	0.87	0.77	0.00	0.02	0.01	0.02	0.03	0.14	1.28	0.75	0.63
ML27	53	1916.4	8.27	4.61	3.66	0	0.04	0.03	0.04	0.07	-28.6	-7.7	-5.4	6.8	0.7	6.1	4.0	1.9		0.19	1.55	0.86	0.69	0.00	0.01	0.01	0.01	0.01	0.13	1.14	0.75	0.36
ML28	55	1910.0	7.70	4.21	3.49	0	0.05	0.05	0.08	0.13	-29.8	-6.9	-3.9	6.6	0.7	5.8	3.0	3.0		0.15	1.18	0.65	0.54	0.00	0.01	0.01	0.01	0.02	0.11	0.89	0.46	0.46
ML29	57	1903.1	7.86	3.28	4.59	0	0.04	0.07	0.07	0.15	-28.9	-7.1	-5.4	6.4	0.8	6.7	4.1	2.6		0.16	1.24	0.52	0.73	0.00	0.01	0.01	0.01	0.02	0.13	1.06	0.64	0.41
ML30	59	1895.7	9.49	5.71	3.78	0	0.06	0.14	0.07	0.21	-29.3	-7.8	-5.4	6.0	0.8	5.5	3.4	2.3		0.12	1.13	0.68	0.45	0.00	0.01	0.02	0.01	0.02	0.09	0.65	0.41	0.28
ML31	61	1887.8	10.08	6.02	4.06	0	0.05	0.07	0.06	0.13	-29.8	-8.6	-5.5	6.0	0.8	5.9	3.6	2.3		0.12	1.26	0.75	0.51	0.00	0.01	0.01	0.01	0.02	0.10	0.74	0.44	0.29
ML32	63	1879.3	8.55	3.83	4.73	0	0.04	0.09	0.04	0.13	-29.8	-9.3	-7.7	6.5	0.9	6.1	4.3	2.8		0.10	0.85	0.38	0.47	0.00	0.00	0.01	0.00	0.01	0.09	0.61	0.42	0.28
ML33	65	1870.2	7.42	1.89	5.53	0	0.10	0.08	0.13	0.21	-29.9	-10.0	-9.1	6.7	0.8	8.1	5.5	1.6		0.10	0.73	0.19	0.54	0.00	0.01	0.01	0.01	0.02	0.08	0.79	0.54	0.16
ML34	67	1860.6	6.74	0.45	6.29	0	0.15	0.06	0.11	0.17	-30.3	-6.8	-4.3	6.7	0.9	8.2	7.4	4.1		0.10	0.69	0.05	0.64	0.00	0.02	0.01	0.01	0.02	0.09	0.83	0.76	0.42
ML35	69	1850.2	8.94	0.46	8.48	0.10	0.22	0.06	0.05	0.12	-31.5	-3.4	-1.2	4.5	1.2	8.2	11.5	1.2		0.06	0.57	0.03	0.54	0.01	0.01	0.00	0.00	0.01	0.08	0.53	0.74	0.08
ML36	71	1839.3	11.25	0.36	10.89	0.32	0.46	0.08	0.06	0.14	-32.0	0.1	3.1	2.6	1.5	8.5	17.0	6.7		0.08	0.87	0.03	0.84	0.03	0.04	0.01	0.00	0.01	0.12	0.65	1.32	0.52
ML37	73	1827.6	12.38	2.43	9.95	0.28	0.34	0.04	0.02	0.06	-30.7	0.5	2.6	2.7	1.5	7.7	15.5	8.2		0.08	0.97	0.19	0.78	0.02	0.03	0.00	0.00	0.00	0.12	0.61	1.22	0.64
ML38	75	1815.1	12.73	2.89	9.84	0.17	0.28	0.10	0.01	0.11	-30.2	-0.1	2.3	2.6	1.5	7.7	13.7	5.9		0.04	0.53	0.12	0.41	0.01	0.01	0.00	0.00	0.00	0.06	0.32	0.57	0.24
ML39	77	1802.0	12.47	1.46	11.01	0.26	0.32	0.05	0.02	0.06	-30.6	-1.5	1.1	2.4	1.4	9.2	14.4	4.8		0.06	0.79	0.09	0.70	0.02	0.02	0.00	0.00	0.00	0.09	0.58	0.91	0.30
ML40	79	1788.0	12.29	1.12	11.17	0.23	0.29	0.05	0.01	0.06	-30.7	-0.7	2.1	2.6	1.5	8.7	16.1	2.9		0.04	0.49	0.04	0.44	0.01	0.01	0.00	0.00	0.00	0.06	0.34	0.64	0.11
ML41	81	1773.2	12.44	2.13	10.31	0.30	0.39	0.06	0.03	0.09	-30.9	-0.8	2.3	2.5	1.5	8.0	19.8	7.3		0.04	0.50	0.09	0.41	0.01	0.02	0.00	0.00	0.00	0.06	0.32	0.79	0.29
ML42	83	1757.6	11.73	1.57	10.16	0.28	0.42	0.09	0.05	0.14	-30.7	-2.5	-0.3	2.7	1.4	8.5	27.0	4.3		0.03	0.39	0.05	0.34	0.01	0.01	0.00	0.00	0.00	0.05	0.28	0.90	0.14
ML43	85	1741.1	10.64	1.75	8.89	0.20	0.27	0.05	0.02	0.07	-30.3	-2.0	0.9	3.0	1.5	6.9	20.5	8.2		0.05	0.54	0.09	0.45	0.01	0.01	0.00	0.00	0.00	0.08	0.35	1.03	0.41
ML44	87	1723.7	13.66	2.31	11.35	0.28	0.39	0.08	0.03	0.11	-30.1	-0.8	1.6	2.7	1.6	8.3	15.9	6.9		0.03	0.43	0.07	0.36	0.01	0.01	0.00	0.00	0.00	0.05	0.26	0.51	0.22
ML45	89	1705.3	14.66	2.71	11.95	0.38	0.44	0.05	0.02	0.06	-30.4	0.3	1.9	2.5	1.8	7.7	15.6	2.5		0.07	1.00	0.18	0.82	0.03	0.03	0.00	0.00	0.00	0.12	0.53	1.07	0.17

Table D: Concentration and isotope data in both unstandardized and standardized form.

CURRICULUM VITAE

Alyssa Nicole Henke

Education

- Master of Science Degree in Geology, Indiana University, earned at Indiana University-Purdue University Indianapolis (IUPUI), November 2020
- Bachelors of Science Degree in Geology, Indiana University, earned at Indiana University-Purdue University Indianapolis (IUPUI), December 2016
- Minor in Mathematics, Indiana University, earned at Indiana University-Purdue University Indianapolis (IUPUI), December 2016
- Minor in Geography, Indiana University, earned at Indiana University-Purdue University Indianapolis (IUPUI), December 2016
- Capstone: Ball State University Geology Field Camp, earned at Ball State University, June 2016

Conferences Attended

- Midwest Geobiology 2016, University of Cincinnati
- Midwest Geobiology 2017, Indiana University-Purdue University Indianapolis (IUPUI)
- Geological Society if America (GSA) Joint Sectional Meeting 2017, Pittsburg PA
- Midwest Geobiology 2018, Northwestern University
- Geological Society if America (GSA) Annual Meeting 2018, Indianapolis IN